Università degli studi di Urbino Carlo Bo

Department of Biomolecular sciences (DISB)

Ph.D. programme in: Biomolecular and Health sciences

CYCLE: XXXVI

Characterization of biological activity and epigenomic remodulation induced by a small-molecule member of hydroxypyrones family in APL blasts

ACADEMIC DISCIPLINE: MED/46

Coordinator: Prof. Marco Bruno Luigi Rocchi

Supervisor: Prof. Mirco Fanelli

Co-Supervisor: Dott. Stefano Amatori

Ph.D. student: Francesco Cantatore

Academic year

2022-2023

TABLE OF CONTENTS

ABBREVIATIONS

AML Acute myeloid leukemia

bp base pair

ChIP Chromatin immunoprecipitation

Ct Cycle threshold

DNMT DNA methyltransferase

FBS Fetal Bovine Serum

GSEA Gene Set Enrichment Analysis

HDAC Histone deacetylase

HKMT Histone lysine methyltransferase

NCI National Cancer Institute

NGS Next generation sequencing

NIH National Institute of Health

OD Optical density

RCF Relative centrifugal force

RPKM Reads per kilobase of transcript per million

RT-PCR Real Time Polymerase Chain Reaction

PCA Principal component analysis

SD Standard deviation

WB Western Blot

ABSTRACT

Over the last few decades, hydroxypyrones and their derivatives compounds have been developed and explored due to their versatility, ability in coordinating metal ions and their potential anti-tumor properties. The epigenomic reprogramming potential of maltonis, a novel maltol-derived molecule with promising antiproliferative activity against leukemic cells, has been investigated in the acute promyelocytic leukemia (APL) NB4 cell line. APL is an aggressive subtype of acute myeloid leukemia (AML), and it is characterized by the oncogenic activities of the PML/RARα fusion protein which recruits repressive complexes to the promoter of specific target genes. Indeed, epigenetic perturbations, as alterations of histone H3 lysine 9 trimethylation (H3K9me3), have been frequently found in AMLs and have been associated with leukemogenesis and leukemia progression.

The data collected in this work that maltonis treatment induces a profound transcriptomic and epigenomic remodulation, resulting in a global reduction of H3K9me3 signal and modulation of other histone post-translational modifications. Further analysis reveals that maltonis exposure induces substantial changes of genes expression (288 upregulated and 551 downregulated genes) in association with the regulation of the permissive histone H3 marks lysine 4 trimethylation (H3K4me3) and lysine 27 acetylation (H3K27ac) at their gene promoters. Maltonis treatment impacts significatively the interferon alpha and gamma response pathways, upregulating them, while downregulating c-MYC target genes. Notably, the unexpected and substantial antiviral-like response triggered by maltonis may hold the key for understanding its mechanism of action, and it may be speculated a potential connection to the widespread reduction of H3K9me3 mark and the consequent dysregulation of repetitive DNA regions.

Collectively, our findings demonstrate the ability of maltonis to reprogram APL cells by epigenetically remodulating their genes expression profile, particularly through the activation of interferon signaling and in the downregulation of c-MYC-related pathways, thus making it an attractive candidate for future clinical applications in anti-leukemic therapy.

INTRODUCTION

Since Hippocrates' first attempts in 2,000 b.C., a lot of efforts have been done over the years to understand the tumor's biology and, nowadays, it still be scratched only the surface of how to fight it. Chemotherapy and radiotherapy are largely diffuse but, over the last decades, the strategies to target cancer have changed to more targeted therapies. Different kinds of targeted therapies have been developed and approved by the Food and Drug Administration (FDA), and a higher number is in development, aiming at different therapeutic targets: Bcl-2 inhibitors, epigenetic inhibitors (e.g., HDAC inhibitors), proteasome inhibitors, kinase inhibitors and many others (Zhong L., *et al.*, 2021). Small molecules are “on the crest of a wave” representing potential new ways of cancer treatment since there is a need for specific therapies that differ from patient to patient. In fact, the constant research for new targets is directly driven from the lack of specific therapies in different cancer subtypes and from the subsequent acquired resistance to chemotherapeutic drugs. These two aspects still represent a limitation that researchers are trying to overcome with more tolerable and higher effective compounds.

In this chapter it will be addressed an introduction to a family of compounds, hydroxypyrones, tested for their potential anti-proliferative and anti-tumorigenic activity; furthermore in the results and discussion sections, it will be discussed in detail one member of this family.

1. Cancer

Cancer represents one of the deadliest and most difficult diseases to treat. It has been estimated by Ferlay J., *et al*. that in 2020, 19.8 million of new cases have arised and 10 million of deaths have happened worldwide (Ferlay J., *et al*., 2021): numbers that, according to a report from the International Agency for Research on Cancer (IARC), are expected to increase dramatically by 2040.

1.1 What drives cancer? - The hallmarks of cancer

The question that emerges spontaneously when approaching a tumor is: what drives cancer? To address this question, it is necessary to consider several crucial points that establish a way to define the required steps for normal cellular transformation, also known as hallmarks of cancer.

Cancer is a very complex disease, in terms of phenotypes and genotypes among different subtypes and it could be promoted by different factors. It is considered a multistep disorder rising from a defective event, as genetic mutations or epigenetic aberrations, and subsequently followed by a cascade of abnormal events leading to malignant cell transformation. These biological changes are not only related with intrinsic factors and other external agents can be involved as:

- ionizing agents, as gamma rays, X-rays, UV radiation;
- chemical agents, as arsenic, tobacco, benzene, nickel, radon;
- biological agents, such as some viral agents (e.g., HPVs, EBVs, HBVs), parasites (e.g., *O. viverrini*) or bacteria (e.g. *H. pylori*) (Wu S., ***et al.***, 2016).

In addition to the role of carcinogens, it is known that the chances of cancer development are higher as age increases, as a result of lifespan extension and reduced function of the cells repair mechanisms (Berben L., ***et al.***, 2021).

To classify the potential of cellular transformation, different functional requirements and capabilities need to be acquired and these have been classified into what are known as hallmarks of cancer (Hanahan D., 2022):

- self-sustaining proliferative signaling by deregulating this signaling, cancer cells acquire the ability to sustain their growth in complete autonomy. They become able to produce their own mitogenic signals or, alternatively, inducing other non-tumor cells to produce it;
- evading growth suppressors activities: in order to sustain their ability to proliferate, cancer cells activate ways to negatively regulate tumor suppressive programs (as RB or TP53);
- resisting cell death: cancer cells master cell death by avoiding apoptotic programs. In this sense they negatively regulate expression of anti-apoptotic proteins (ex. Bcl-2 family), autophagy machinery component (TGF-β) and inducing necrosis factors to promote tumor (ex. releasing IL-1);
- enabling replicative immortality: to sustain tumor growth, cancer cells acquire limitless replicative potential, through the telomere maintenance, by telomerase activity, and by suppressing cellular senescence pathways;

- inducing angiogenesis: upregulation of factors involved in inducing angiogenesis, as vascular endothelial growth factor-A (VEGF-A), and preventing expression of those inhibiting it, as thrombospondin 1 (TSP-1). By this, cancer cells sustain growth with the sufficient afflux of nutrient and oxygen, mimicking a normal tissue;
- activating invasion and metastasis: cancer cells acquire the ability to invade, enhance cell motility, express protease to degrade extracellular matrix and disseminate from a primary tumor to another site in the body. This, mainly, is associated with downregulation of E-cadherin expression, a well-established protein involved in cell-to-cell junctions;
- deregulating cellular energetics: to fuel cell growth and division, cancer cells need to push their proliferation by glycolytic switch, that allows for a generation of different intermediates of biosynthetic pathway, facilitating production of macromolecules;
- genome instability and mutation: this step is fundamental, both for acquisition and progression of tumor capabilities. Defects in “DNA caretakers” result in loss of their function by inactivating mutation or epigenetic repression;
- avoiding immune destruction: immune evasion represents one of many forms of cancer cells to conceal eradication by disabling component of the immune system (e.g., secretion of immunosuppressive factors, as TGF-β);
- tumor-promoting inflammation: inflammatory response is a way by which cancer cells can achieve hallmarks and evade suppression by the immune system. Moreover, immune response cells can release some reactive oxygen species (ROS), that are actively mutagenic with nearby cells (Hanahan D. and Weinberg R., 2011).

Recently, new additions have been made to this list of characteristics by Hanahan D., corresponding to:

- unlocking phenotypic plasticity: critical component to bypass terminal differentiation. Cancer cells can “unlock” this capability by three different ways: de-differentiation (when differentiated cells reverse to a progenitor cells), blocked differentiation (from progenitor cells), trans-differentiation (differentiated cells can show a new phenotype of another lineage cell);

- non mutation epigenetic reprogramming: gene expression can be directly regulated by epigenetic modifications. This becomes relevant in the context of carcinogenesis because the tumor microenvironment can directly influence the epigenome;
- senescent cells: considered for a long time as a protective mechanism, it has been demonstrated that in some of these types of cells can stimulate cancer by producing a plethora of bioactive factors, contributing to proliferation instead of preventing it (Lee S. and Schmitt CA., 2019);
- polymorphic microbiomes: some variation of specific microbiomes (e.g., intestine), could raise species of bacteria that have been reported to enable the expression of hallmarks of proliferation, as for example in colon epithelium (Okumura S., *et al.*, 2021).

These peculiarities highlight parameters, often interconnected one to another, to understand cancer biology and pathogenesis (Figure I). Thus, it is not surprising that these multiple hallmarks can be coordinated directly by oncogenic drivers, such as KRAS or c-MYC (Hanahan D., 2022).

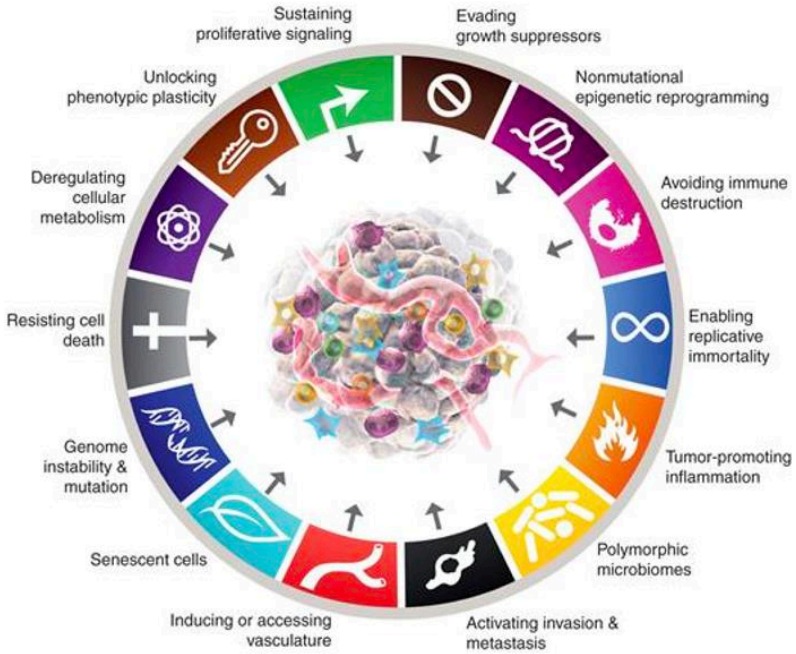

Figure I. All biological hallmarks acquired from cancer cells that define the transformation of a normal cell in a cancerous cell, updated in 2022 (Hanahan D., 2022).

1.2 The handyman gene: *MYC*

c-MYC is a global transcription factor belonging to the family of helix-loop-helix leucine zipper (bHLHZip) proteins, which can dimerize with another bHLHZip protein, MAX, to form a complex interacting with specific DNA sequence to regulate a plethora of genes. c-MYC carries out many different functions in the cells: from cell proliferation, metabolism, DNA damage response, transcription and many more as reported in Figure IIA (Pelengaris S., *et al.*, 2002).

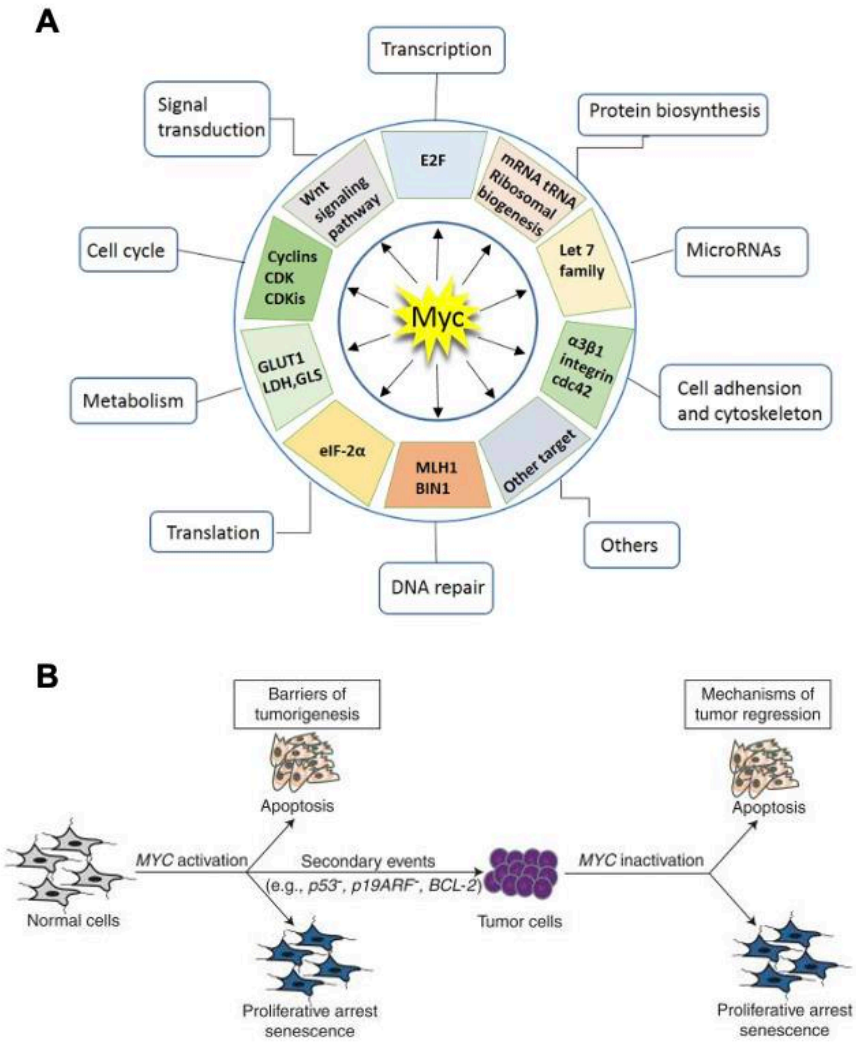

Figure II. A. Transcription factor c-MYC has multiple function within cells. It is involved in many processes from transcription, translation, cell cycle regulation, metabolism and many more (Chen H., *et al.*, 2018). **B.** c-MYC activation in normal cells is not enough for tumorigenesis, who needs a boost of secondary events (as p53 mutation or Bcl-2 expression) for a neoplastic transformation (Gabay M., *et al.*, 2014).

c-MYC is also involved in hematopoiesis and maturation of myeloid and lymphoid cells, where its uncontrolled expression could lead to hematological malignancies (Ahmadi S.E., *et al.*, 2021). According to this, *MYC* gene is regulated through many pathways and positive loop feedback while c-MYC protein expression is tightly regulated by cells through a rapid proteasomal degradation. Its deregulation represents a key event in many cancer types and can be promoted by chromosomal rearrangements, retroviral infections and super-enhancers activation. In fact, as mentioned in the previous section, overexpressed c-MYC can be considered an oncogenic driver for tumor cells to enhance proliferation (Madden S.K., *et al.*, 2021).

As shown in figure II B, a paradox arises: *MYC* overexpression alone is incapable of inducing proliferation and this is supported also by the fact that in normal cells, this event directs cells to proliferative arrest, inducing senescence and/or apoptosis (Gabay M., *et al.*, 2014; Nilson JA. and Cleveland JL., 2003). Another important feature to keep in consideration is that c-MYC oncogenic activity depends on the development state of cells, meaning that also the epigenetic and genetic state of cells are crucial to define their fate (Beer S., *et al.*, 2004).

Oncogenic c-MYC is considered to coordinate 40% of all tumors: the most known is Burkitt's lymphoma, an aggressive blood cancer type in which a chromosomal translocation that boosts c-MYC expression occurs (Molineaux M. E., *et al.*, 2012; Miller D. M., *et al.*, 2012). In breast cancer, c-MYC expression is amplified, coupled with breast cancer associated 1 (BRCA1) tumor suppressor and in estrogen receptor (ER) inhibition (Xu J., *et al.*, 2010).

In colorectal cancer, oncogenic c-MYC is able to reprogramme global metabolism and, specifically, by negatively regulating mitochondrial biogenesis (Satoh K., *et al.*, 2017).

Moreover, it is not surprising that most of the research group's efforts are oriented in targeted therapies to find a way to drug c-MYC. Indeed, among different strategies, from peptides (e.g., Omomyc) to small molecules (e.g., 10058-F4), the lack of a therapeutic approach to target c-MYC in clinics is challenging and with new insights on how some types of cancer work, designing new drugs towards inhibiting c-MYC will reach new milestones (Madden S., *et al.*, 2021; Hoffman B., *et al.*, 2002).

1.3 Hematological malignancies

Among different types of cancers, one of the most aggressive is represented by blood cancers. The World Health Organization (WHO) classifies hematological malignancies based on lineage, morphology, phenotype, clinical features and it comprises leukemia, myeloma, chronic lymphoma, myeloproliferative disorders and myelodysplastic syndromes (Rodriguez Abeu D., *et al.*, 2007; Khoury J.D., *et al.*, 2022).

These types of hematological cancers start in bone marrow, where normally hematopoietic cells are produced, or in immune system cells. In detail, in leukemias, bias during differentiation of hematopoietic stem and progenitor cells through a lymphoid or myeloid cells path, result in a process of leukemogenesis, where a clone acquires an advantageous mutation that could result in the development of leukemia (von Beck K., *et al.*, 2023).

Specifically, the most lethal hematological malignancy is represented by leukemias, a heterogenous group of disorders associated with an increased number of leukocytes in blood or bone marrow deficit in normal production of blood cells.

The global burden of hematological malignancies has estimated that the frequency of this type of blood cancer is higher in western Europe and North America (Zhang N., *et al.*, 2023).

The overall cases have increased in all types of leukemias from 1990 and it has been estimated, in 2018, an increment of almost 500,000 new cases, with a major incidence in males and variability within age, slightly increased in patient over 65 years (Dong Y., *et al.*, 2020).

Leukemias are classified based on two parameters:

- rate of progression, which could be divided into:
  - ◊ acute, which represent a category where cells multiply quickly, form blasts from immature cells and, if not treated rapidly, they can spread all over the body;
  - ◊ chronic, represented by defects in white blood cells. Unlike the acute, chronic leukemias are usually slower and require more time also to evaluate the treatment to use.
- types of progenitor cells path:
  - ◊ myeloid leukemias, involving red blood cells, platelets and some white blood cells as granulocytes and monocytes;

◊ lymphoid leukemias, associated with primary white blood cells, as lymphocytes.

By considering these two possible ways to classify them, leukemias can be distinguished into 4 main groups:

- Acute Myeloid Leukemia (AML)
- Chronic Myeloid Leukemia (CML)
- Acute Lymphocitic Leukemia (ALL)
- Chronic Lymphocitic Leukemia (CLL)

Among those types, AML has gained particular attention over the years, due to its lethality, with younger people, and heterogeneity (Dönher H., *et al.*, 2022). The WHO has classified a huge number of subtypes of AML, each one related to a different subset of events occurring and favorable to the patient's classification.

Generally, AML are classified into:

1. AML with chromosomal abnormalities, with the most known types being the PML-RARα or the MLL-AF9 fusion gene types of AML;
2. AML with cytogenetic mutations, also known as myelodysplastic syndrome, in which a mutation can develop, for example on NPM1 gene;
3. Therapy-related AML, with a unique development when negative response to therapy occurs (Arber A., *et al.*, 2016; Taylor J., *et al.*, 2017).

Indeed, as reported by Dönher H., *et al.*, 2022, the diagnosis is based on different levels, from the rapid screening test to establish diagnosis through immunophenotyping by flow cytometry or genetic screening of prognostic markers (RUNX1, FLT3, PML-RARα) and medical history (e.g., predisposition).

Advances in sequencing techniques and approaches to study cancer, have revealed other aspects to be investigated like epigenetics dysregulation. Substantially, in AML, epigenetics aberrations, as DNA methylation or alterations of histone modifications, are considered a new hallmark for the cancer progression and many have been identified as crucial events in the hematopoiesis and differentiation (Fennel A.K., *et al.*, 2019).

These aspects will be reprised in the next chapter, but it is undoubtful that by targeting these epigenetic features, it will represent a new way to develop more effective treatment strategies and improve outcomes for patients with AML.

1.4 State of the art of cancer therapies

Cancer therapy refers to the various treatment approaches and techniques used to manage and potentially cure cancer. The goal of cancer therapy is to eliminate cancer cells or control their growth, relieve symptoms, prolong survival, and improve the quality of life for individuals diagnosed with cancer (Smith J., *et al.*, 2021).

The canonical way to treat cancer remains related to surgery, radio- and chemotherapy and in some types of cancers this is still the best approach (Weinberg R., *et al.*, 2014).

Otherwise, chemotherapy is unable to target specific cancer cells and this could enhance toxicity to some treatments. Thus, new approaches in the last few years have revolutionized cancer treatment, and among those, targeted therapy using small molecules has arised to grant a more specific and low toxicity treatment (Zhong L., *et al.*, 2021).

Targeted cancer therapy is an innovative approach that focuses on specific molecular targets within cancer cells, aiming to disrupt their growth signals and promote cell death while minimizing damage to healthy cells. Unlike conventional chemotherapy, which affects both healthy and cancerous cells, targeted therapy utilizes drugs that selectively act on the genetic mutations or abnormal proteins that are unique to cancer cells (Brown L., *et al.*, 2021).

These drugs can be monoclonal antibodies or small molecule inhibitors that interfere with key signaling pathways involved in cancer development and progression.

Many drugs have been approved by FDA and entered in clinics during these years, starting from the approval of imatinib, a tyrosine-kinase inhibitor, in 2001.

Among those several small molecules, it can be distinguished based on their mechanism of action (Figure III):

- alkylating agents, drugs that commonly present an unstable alkyl group who reacts with protein and DNA. Inhibit replication and transcription (e.g., platinum analogs, cyclophosphamide);

• antimetabolites, these drugs inhibit DNA replication. Among those it can be found molecules as 5-azacitidine, methotrexate, 5-fluorouracil;

• antimicrotubular agents, principally involving topoisomerase inhibitors (daunorubicin, topotecan) and mitotic spindle inhibitors (taxanes, vincristine);

• miscellaneous, drugs not corresponding to a specific category, in which it can be found proteasome inhibitors, arsenic trioxide or hydroxyurea;

• antibiotics, the function of this is to inhibit RNA and DNA synthesis, e.g., actinomycin D;

• immunotherapy, monoclonal antibodies that unleash immune cells to target cancer cells (as PD-1/PD-L1 antibody Atezolizumab or CTL4 antibody Ipilimumab).

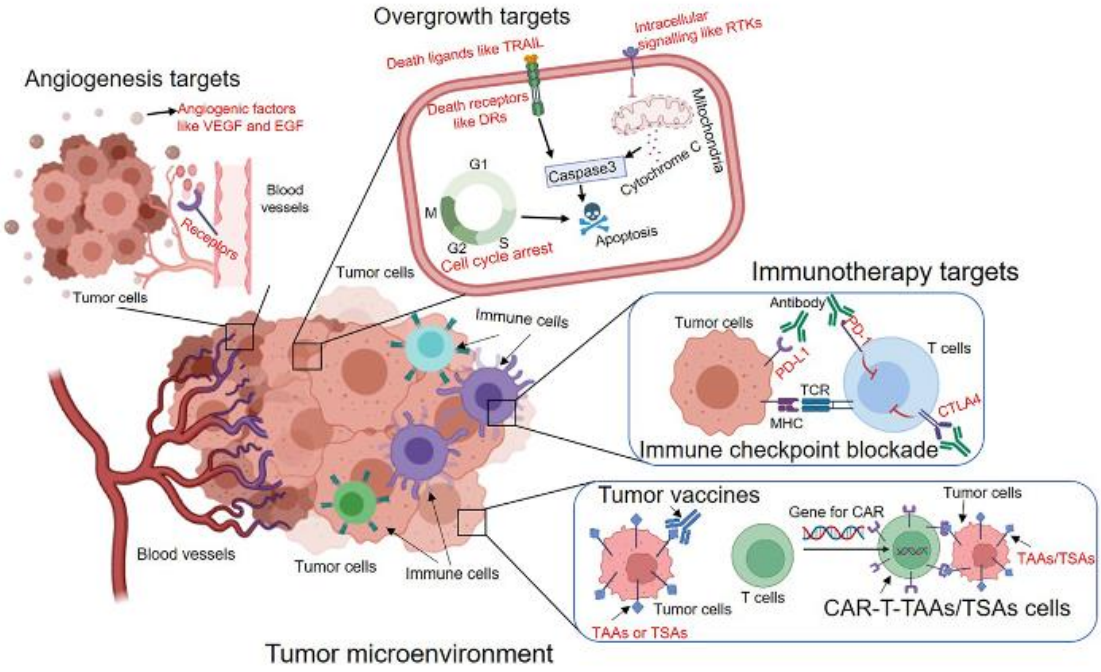

Figure III. Diagram representing principal targets for therapies to inhibit different tumor hotspots, as angiogenesis, overgrowth and immunotherapy. Signed in red are potential pathways targeted by actual cancer therapies (Hou Jue, *et al.*, 2022).

Targeted therapy has shown promising results in various cancer types, including breast, lung, colorectal, and melanoma. It has the potential to provide more effective and personalized treatment options, improving patient outcomes and minimizing side effects (Doe J., *et al.*, 2023). Beneath those types of approaches, it is worth to mention the epigenetic-based therapies, so specific types of compounds interacting with chromatin remodelers (entinostat, HDAC inhibitor)

or DNA (as decitabine, DNMT inhibitor) have been developed and already approved in clinics, as a peculiar treatment for some kind of AML (Fennell K.A., Bell C.C. and Dawson M.A., 2019). Despite the specificity of these new approaches to fight cancer, currently, the major challenge is drug resistance. This mechanism is linked to gene mutations, epigenetic remodeling, apoptosis disruption etc. that happens across time. Another important challenge is referred to low efficiency, in terms of patients in which the drug is effective and along this, it remains crucial to continue the identification of new predictive biomarkers.

To contrast those challenges, many strategies have been developed, from combinational therapy, such as antibody-drugs therapy, to multitarget drugs or combination of two compounds for epigenetic-based therapies (Fennell K.A., Bell C.C. and Dawson M.A., 2019). Thus, it is fundamental to deep understanding of tumor biology and alongside the evolution of new strategies and techniques, the small molecules will continue to represent the major font of treatment for cancer, side by side with immunotherapy, and they will be the gold standard for therapies in the near future.

2. Epigenetics

The term “epigenetics” has emerged since 1942 with the biologist Conrad Waddington declaring that “it refers to events able to regulate the process of development from oocytes to mature organisms”. Afterwards, in the last 30 years, it was gained more insights about what epigenetics represents and now it is recognized as “the reversible changes that does not occur on DNA and modulate the expression of a particular genotype in a specific phenotype” (Allis C. and Jenuwein T., 2016).

Indeed, epigenetics controls the fate of a stem cell and this commitment is inherited through what is defined as “epigenetic memory”, which defines a specific gene expression profile in a differentiation pattern of a cell.

The complex genomic organization of eukaryotic cells resides in the highly organized structure mediated by chromatin, constituted by nucleosomes. Nucleosomes are histone octamers where 147 base pairs of DNA are wrapped around them and then chromatin is packed to form chromosomes (Figure IV).

Chromatin structure is dynamic and, based on the state, it regulates gene expression through accessibility to transcription factors. Indeed, two distinct forms of chromatin can be distinguished:

- constitutive heterochromatin, found in 10 % of nuclear DNA and representing the highly condensed chromatin, mainly located in telomeric, pericentromeric and centromeric regions;
- euchromatin, along the facultative heterochromatin, is represented by 90% of the genome and it is more relaxed.

Further, the part of the genome that is associated with open chromatin, containing the majority of actively expressed genes, is represented by a small fraction of the 2-3% (Thurman R., *et al.*, 2012). These dynamics of chromatin accessibility is strictly related to the occupancy of nucleosomes on DNA and, indeed, this depends on a series of factors like epigenetics modifications, cell status, transcription factors and chromatin architectural proteins (as CTCF, cohesin, SWI-SNF complex etc.) (Klemm S.L., *et al.*, 2019).

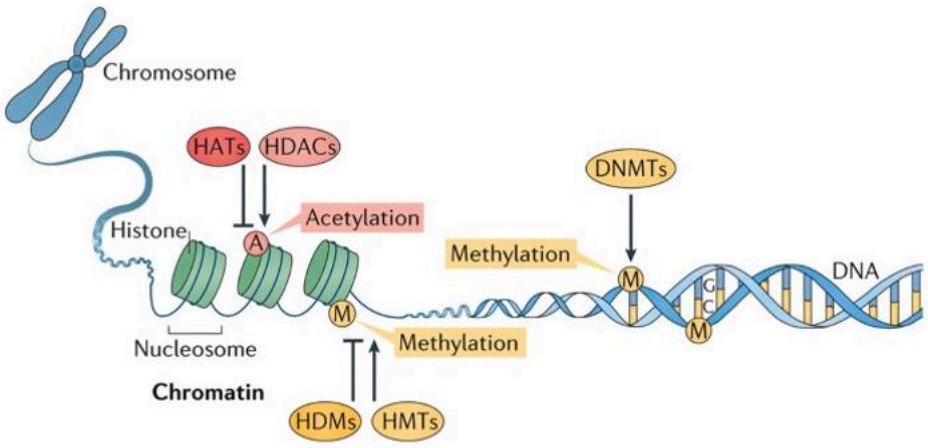

Figure IV. Overview representation of genome complexity, where DNA elics is wrapped and packed with histone proteins to form chromatin. DNA and histones could undergo in different chemical modification that makes the structure highly dynamic and able to regulate gene expression. (Niederberger E., *et al.*, 2017).

Furthermore, epigenetics modification can be distinguished between those of histone proteins (histone modifications, e.g., methylation or acetylation) and those happening on DNA

sequences, where the sequence is not changed but there is a transfer of a chemical group on nucleotides (Figure IV).

These marks are inherited through a mechanism of semiconservative replication, where histones are recycled or *de novo* added during the process of replication and it seems to involve many players, as chaperones or nucleosome remodelers, linked to the DNA replication machinery (Almouzni G. and Cedar H., 2016). Indeed, for these epigenetics modifications it is important to distinguish between different players able to shape chromatin and that have been identified as epigenetic modifiers of chromatin. These are divided in three categories, representing respectively of writers (the one who introduce modification to a specific site), readers (able to identify the modification through a specific domain) and erasers (enzymes who are capable of removing the chemical tag from a specific site) (Tarakhovsky A., 2010).

In addition to these cellular aspects, there are several factors that could influence the epigenetics patterns of cells, all related to lifestyle impact. Thus, a plethora of common things shaping the epigenetics mechanisms have been assessed, as environment, age, diet, exercise, habits and gender (Bar-Sadeh B., *et al.*, 2020).

2.1 DNA methylation

DNA methylation was first discovered in mammals in the early 50s, where modified cytosines were found to be in a nonrandom distribution through paper chromatography on calf thymus (Mattei A., *et al.*, 2022).

DNA methylation is a post-replication epigenetic modification of genomic DNA, in which a methyl group ($-CH_3$) is added to a cytosine and adenine bases, but mainly at CpG di-nucleotide motifs. Of note is that first in plants and then in human embryonic stem cells, this modification has been identified in non CpG context sites (Jin B., *et al.*, 2011). This modification is catalyzed by a group of proteins called DNA methyltransferase (DNMTs), which add a methyl group from the intermediate S-adenosylmethionine (SAM) to the cytosine (Figure VA). Among this family, have been reported several proteins: DNMT1, DNMT2, DNMT3 (a, b, c), DNMT3L. However, only DNMT1, DNMT3a and DNMT3b carry the methyltransferase activity. In addition, DNMT1 is

associated with maintenance of methylation signature during replication, while DNMT3a and 3b with *de novo* methylation (Moore L.D., *et al.*, 2012).

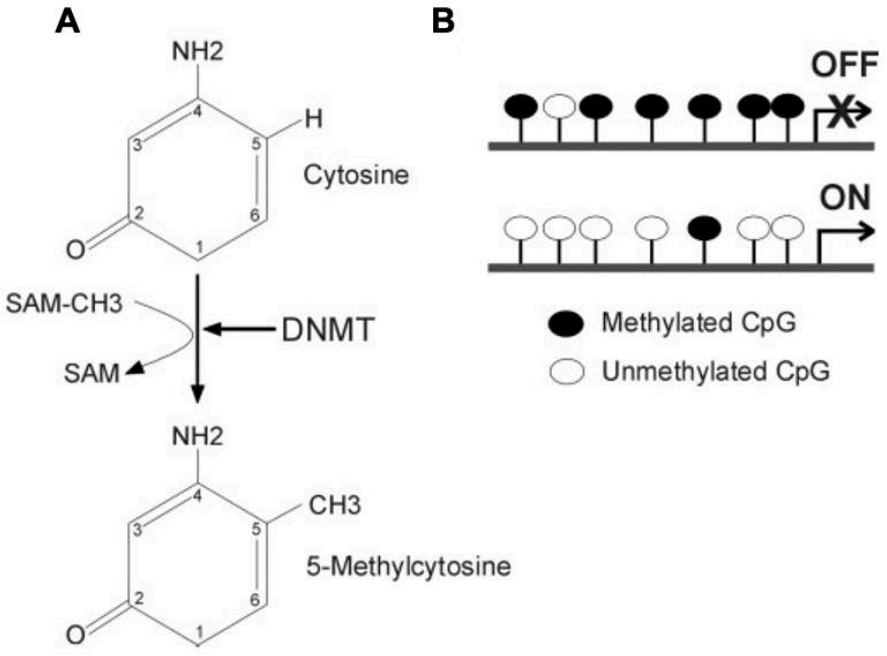

Figure V. A. DNA methylation mechanism of cytosine conversion into 5-methylcytosine, where DNMTs mediate the transfer from SAM to cytosine and **B.** effect of DNA methylation on gene expression at CpG islands of promoter genes (Collas P., Noer A. and Sørensen A.L., 2008).

This modification was identified to be stable and heritable through generations, especially for the key role in imprinting the methylation at specific genes loci during embryonic development, and for other biological processes, including transcriptional regulation, X-chromosome inactivation and transposon silencing (Riggs A.D. and Xiong Z., 2004; Zeng Y. and Chen T., 2019).

Indeed, one main contribution of DNA methylation is represented by transcriptional regulation, in which methylation at CpG site at promoter region can directly recruit methyl-CpG binding domain (MBD) who can help remodel of the site and regulate the binding of transcription factors, by that, turning the gene off or on depending on the methylation level (Figure V B).

This regulation system is a key feature, frequent object of dysregulation in cancer, where tumor suppressor genes are silenced in the early steps of cancer development (Di Croce L., *et al.*, 2002; Turpin M. and Salbert G., 2022).

Recently, another feature detected in plants and to be further analyzed in mammals, is represented by the fact environmental stress can cause epigenetic remodeling of gene expression and mainly through DNA methylation upregulation (Kumar M. and Rani K., 2023).

Besides being a stable modification, preventing differentiated cells to revert in stem cells, methylation on genomic DNA can be reverted passively through cell division or actively, by active DNA demethylation agents. This process of removing the methyl group from 5-meC to cytosine is mediated through dioxygenase TET proteins, occasionally by base excision repair (BER) or deamination of 5-meC to T followed by BER on mismatch T-G (Wu S.C. and Zhang Y., 2013; Wu X. and Zhang Y., 2017).

Another way to remove methylation is through incorporation of 5 azacytidine, a chemical analog of cytidine, in DNA strands during replication and preventing the action of DNA methyltransferases. This small molecule is largely used in clinics, as FDA approved chemotherapeutic, for treatment of patients with myeloid malignancies (Gang A. O., *et al.*, 2014).

All things considered, although the developed sequencing techniques, gaps remain in our knowledge of DNA methylation and future studies will aim to enrich our understanding of how, when and where DNA is methylated.

2.2 Histones and histone post- translational modifications (HPTMs)

Histone proteins are expressed in bacteria, archaea and eukaryotes; however these last two domains share some structural analogy and function, evolutionary linking eukaryotes to the archaeal branch (Henneman B., *et al.*, 2018). Specifically, eukaryotic histones are found in cell nuclei and they are the core component of nucleosomes, the basic structure of chromatin.

Histones are classified into five different group of proteins: H1, H2A, H2B, H3 and H4 where two pair of the histones variant H2A, H2B, H3 and H4 are the component of the histone octamer,

instead histone H1 is known as a linker histone connecting one nucleosome to another (Amatori S., *et al.*, 2021).

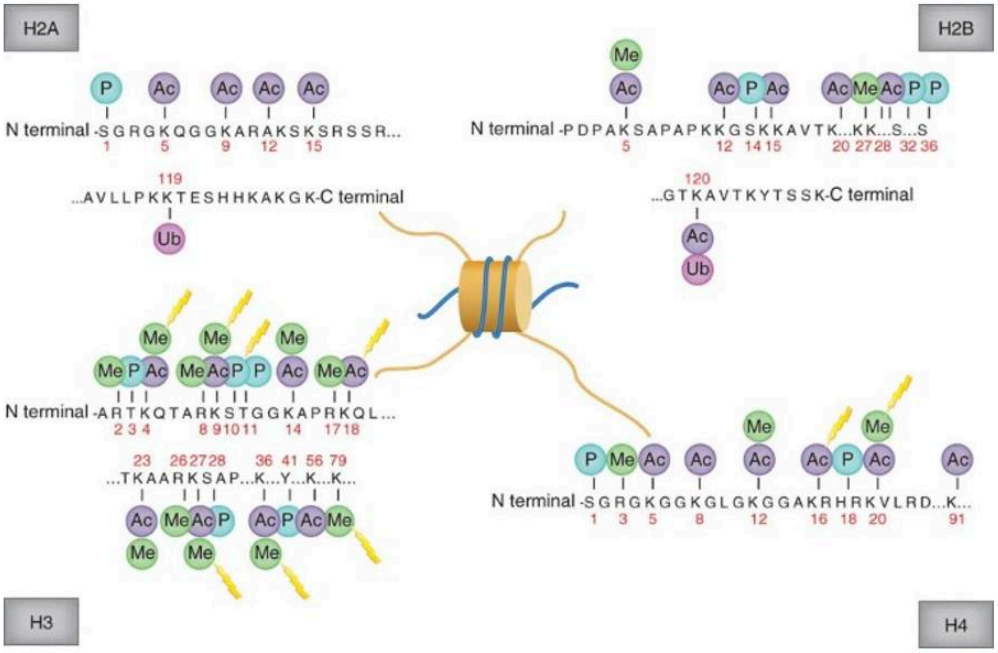

Figure VI. The figure depicts the main and most studied modifications along histone tails of the four core histones H2A, H2B, H3, H4 (Rodriguez-Paredes and Esteller, 2011).

These histone variants share a highly conserved structure, with N-terminal tails that are enriched with lysine and arginine residues and where histone post-translational modifications occur (HPTMs).

For this reason, it has been suggested the “histone code”, where post-translational modifications happening on histone tails on different amino acid residues, coupled with DNA methylation, regulates DNA transcription through actual or potential transcriptional states. Moreover, this regulatory mechanism holds the ability of changing a person’s phenotype without modifying the genetic information as, for example, it is happening between twin brothers and sisters (Jenuwein T. and Allis C.D., 2001).

HPTMs, as specified for DNA methylation, do not affect DNA nucleotides, instead they modify the accessibility to a site for the transcriptional machinery. Among those modifications, it can be found the most common methylation, acetylation, phosphorylation, SUMOylation and

ubiquitination that take place on several amino acids and many can accept multiple tags (Figure VI). These modifications manage the chromatin state in specific loci through the switch between open and closed state, mentioned above, to regulate various biological processes in terms of DNA repair, transcription, gene expression, metabolism, chromosome condensation and spermatogenesis (Alhamwe A.B., *et al.*, 2018).

In addition, there are several modifications arised in the last few years with the new high sensitivity standards set in the proteomics techniques, involving short Lys acylation, as for example crotonylation, formylation, benzoylation, propionylation all found linked to transcriptional activation (Ntorla A. and Burgoyne J. R., 2021).

Among HPTMs, the most representative and studied are methylation and acetylation. Histone methylation is mainly occurring in lysines and arginines residues, where methyl groups can be added in two different ways based on the amino acid by histone methyltransferases (HMTs); lysines can be mono-, di-, tri-methylated, otherwise arginines can be mono-, symmetrical or asymmetrical di-methylated (Bannister A.J. and Kouzarides T., 2011). The most studied are lysines methylation sites on histone H3 tail including H3K4, H3K9, H3K27, H3K36, H3K79, whereas the methyl groups addition is catalyzed by HKMTs from SAM to a lysine ε-amino group (Greer E. L. and Shi Y., 2012). As an example, of crucial importance is the H3K27me3 modification, that is a mark of facultative heterochromatin bound by polycomb group of proteins (PcG) (Chammas P., Mocavini I. and Di Croce L., 2020).

Focusing on specific HPTMs associated with this research project, three histone marks were considered: the first is a transcriptional repressive mark associated with heterochromatin, H3K9me3, which is widespread distributed along the genome by SETDB1 methyltransferase and mainly at constitutive heterochromatic regions, pericentromeric and centromere, where is essential for correct chromosome segregation (Sidhwani P. and Straight A.F., 2023). This mark is also epigenetically remodeled in germline and in early embryonic development at imprinting control regions, being established for lineage-specific differentiation (Buckberry S., *et al.*, 2023). H3K9me3 has become attractive from a clinical point of view since its relevance in cancer and cancer resistance was observed, where high levels of the mark are associated with worst

outcomes and key molecular mechanisms in hematological malignancies (Monaghan L., *et al.*, 2019; Gaggioli V., *et al.*, 2023).

Methylation is not only related to silencing, in fact the second mark investigated was the permissive H3K4me3, which is associated with euchromatin regions and deeply involved in a lot of functions, principally transcriptional activation. In detail, this mark is one of the most studied for its role in gene expression and enrichment at transcription start site (TSS), where it has been demonstrated to have a role in regulating RNA polymerase II pause-release (Wang H., *et al.*, 2023). Some experimental evidence have supported the idea that this mark could be fundamental in establishing process of memory of previous chromatin states and transcription consistency and dynamics between cells (Liu X., *et al.*, 2016; Howe F., *et al.*, 2017).

The second most studied and dynamic modification, correlated with euchromatin state, is acetylation, where histone acetyltransferases (HATs) through acetyl-CoA, as cofactor, catalyzes the transfer of the acetyl group to the lysine ε-amino group. Nonetheless, differently from methylation, this modification grants less positive charge to lysine and, by doing so, reduces DNA-histone interactions. The most investigated modification, and third subject of the study, was the permissive mark H3K27ac. This mark is promoted by trithorax group of protein (TRX) and antagonize PcG proteins, and it is principally poised at enhancer sites (Creyghton M.P., *et al.*, 2010).

Intriguingly, it has been found that broad H3K27ac domains overlap with H3K4me3 at TSS sites and its function associated to gene activation, even though the distal peaks of H3K27ac alone characterized putative active enhancers whose nearby genes are expressed at higher level, also during embryogenesis, compared to others (Wu K., *et al.*, 2023). Deregulated acetylation, resulting in hyperacetylation or hypoacetylation, is associated with cancer development and targeting HATs or HDACs have become a new strategic therapy in some tumor type, as hepatocellular carcinoma (HCC) or neuroblastoma (Durbin A.D., *et al.*, 2022).

3. The family of hydroxypyrones

Hydroxypyrones are a family of compounds known for their versatility and their capability of interacting with ion metals, making them a powerful tool for contrasting disorders of metal metabolism, as well as good candidates for newly formulations in metallo-pharmaceutical (Toso L., *et al.*, 2013).

The main chemical structural features of these families are represented by the heterocyclic core and by a hydroxyl group (-OH) in *ortho* position, comprising several positions to attach backbones (2-, 5-, 6-) (Figure VII A).

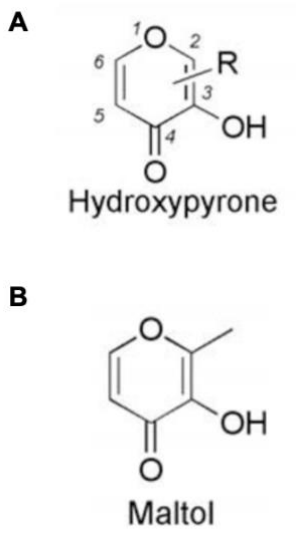

Figure VII. Schematic structures of **A)** hydroxypyrone, and **B)** the most known natural molecule member of the family maltol (Yan Y. L., *et al.*, 2009).

A huge advantage of these molecules is that they are cheap and easy to produce. Moreover, they result to be stable and, in many cases (e.g., aluminum related disease), can be also charged with ions such as Fe^{3+}, Al^{3+}, Cu^{2+}, Ga^{3+} and others, neutralizing charges through their chelation capability (Thompson K.H., *et al.*, 2006).

Nowadays, these compounds are worldwide used for multiple purpose: the investigation principally is posed on formulating metallo-enzymes inhibitors, as histone deacetylases, tyrosinase and metallo-β-lactamase; on the other side many more targets are taking in consideration, starting from the anti-neoplastic characteristics of some members (e.g.,

Deferiprone) and improving in metal ion absorption or distribution, to new fields as anti-dermatophytic agents (Arshad J.Z. and Hanif M., 2022; Karakaya G., *et al.*, 2022).

3.1 Maltol and maltol-derived compounds

Maltol (3-hydroxy-2-methyl-4-pyrone) shown in figure VII B, is a member of the family of hydroxypyrones, known for its bioavailability, acid-base properties and favorable toxicity *in vitro*. Principally, it is found in the bark of some trees, in the pine needles and in roasted malt. Besides the largely application of the molecule as flavor enhancer in the food industry, maltol is used also in cosmetics and pharmaceuticals industries (Harvey R.S.J., *et al.*, 2003; Mohamed A.A. and El-Kadi A.O.S., 2007).

Due to its properties, shared with other members of the family such as kojic acid, maltol is a good choice for develop new biological compounds and it can coordinate several metal cations (e.g., Fe^{3+}, Ga^{3+}, Al^{3+}), with these maltol-derived complexes showing potential anti-tumor characteristics (Dömötör O., *et al.*, 2014). Indeed, ferric maltol is a maltol derived compound approved by FDA for the treatment of patients with iron deficiency, with or without anemia (Schdmit C., *et al.*, 2021).

In addition to already mentioned properties, maltol was found to possess ROS scavenger activity and antioxidant properties, alongside anti-apoptotic and anti-neoplastic activities, providing an attracting molecule to use as the core unit of newly compounds (Murakami K., *et al.*, 2006; Barve A., *et al.*, 2009).

Thus, considering the synthetic versatility of the molecule, many compounds have been designed and tested during the last decades. Among those variants, ruthenium or oxovanadium complexes with maltol, have shown some promising anti-proliferative ability against osteosarcoma cell lines, even if the oxovanadium-maltol complexes were developed mainly for enhancing insulin uptake for treatment of type 2 diabetes mellitus (Saatchi K., *et al.*, 2005; Kandioller W., *et al.*, 2009; Léon I.E., *et al.*, 2014).

Another hydroxypyrone derived molecule called deferiprone, it was developed in 1981 as iron chelator for thalassemia treatment, exhibiting highly bioavailability, low toxicity and also anti-tumoral activity in cancer stem cells (Fiorillo M., *et al.*, 2020). Recently it was proposed as an

inhibitor of demethylation, since in breast cancer cells it demonstrated to suppress demethylation on histone H3K4me3 and H3K27me3 through lysine demethylase 6A (KDM6A) inhibition (Khodaverdian V., *et al.*, 2019).

3.2 Exploring the family of hydroxypyrones derivatives: bis-maltolate small molecules

The constant research of available molecules to use in cancer treatment have brought new questions regarding the exploration of naturally derived compounds such as maltol. The research group of Prof. Vieri Fusi (Dept. of Pure and Applied Sciences, Urbino University) together with the one of Prof. Mirco Fanelli (Dept. of Biomolecular Sciences, Urbino University), have explored a new class of maltol-derived compounds coupled with poly-alkylamine and bivalent ions (Fanelli M. and Fusi V., 2010).

Among those tested, the first molecule that has been selected for its biological activity is the N,N'-bis((3-hydroxy-4-pyron-2-yl)methyl)-N,N'-dimethylethylendiamine, or also known as malten (Figure VIII A).

This bis-maltol-derivative was tested in different solid and hematopoietic cell lines, showing a dose-dependent reduction of cell survival in 72h of exposure and cell cycle perturbations (Amatori S., *et al.*, 2010).

In addition, it was demonstrated that it can induce expression of genes related to apoptosis and cell cycle arrest. To accomplish this effect, it has been proposed that malten is able to form a complex with DNA through intermolecular crosslinking, changing its structure in both cell-free and *in vitro* assays (Amatori S., *et al.*, 2010). This data was corroborated by the fact that single components of malten molecules were not able to induce those changes on DNA, confirming that this action was peculiar to malten.

Other compounds, as *N*,*N*′-bis((3-hydroxy-4-pyron-2-yl)methyl)-1,4-piperazine (L1) and *N*,*N*′,*N*′-tris((3-hydroxy-4-pyron-2-yl)methyl)-*N*-methylethylendiamine (L2) were synthesized as malten derivatives, respectively being two and three maltol molecules conjugated with diamine (Figure VIII B). These two compounds have shown highly affinity for Cu(II) and Co(II), acting as metallo-

ligand and showing different biological behaviors: L1 activity was similar to malten, but not as effective as it, and L2 was able to induce single strand breaks (Macedi E., *et al.*, 2020).

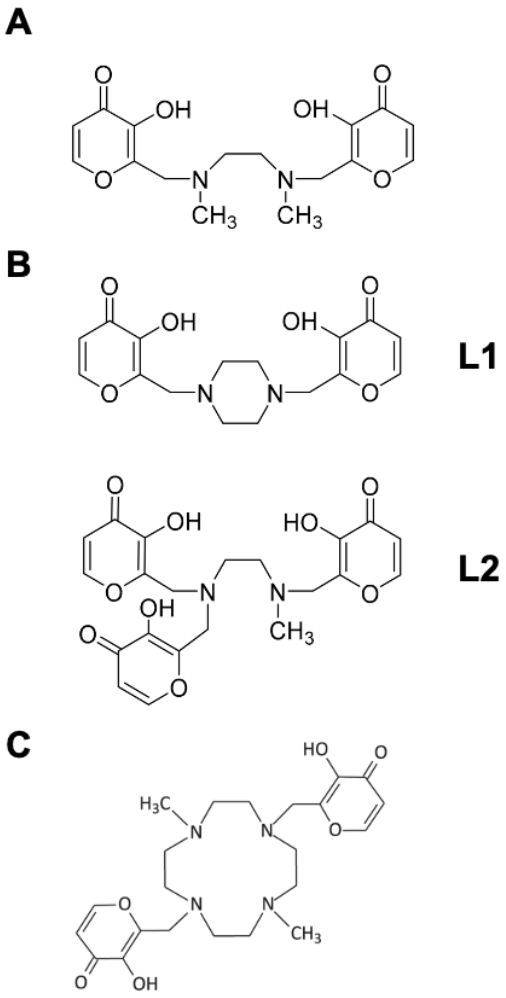

Figure VIII. A) Malten chemical structure with two maltol arms linked by polyamine, **B)** L1 and L2 compounds deriving from malten and **C)** maltonis chemical structure, different from malten due to the presence of the cyclic aliphatic spacer (adpated from Macedi E., *et al.*, 2020).

3.3 Exploring the family of hydroxypyrones derivatives: maltonis

In the continuous experimentation of new combinations to find new effective compounds, a new maltol-derived molecule with a cyclic aliphatic spacer was selected: [4(N),10 (N)–bis[(3-hydroxy-4-pyron-2-yl)methyl]-1, 7-dimethyl-1, 4, 7, 10 tetraazacyclododecane], or maltonis (Fanelli, M., and Fusi, V., 2010) (Figure VIII C). The process of synthesis starts from maltol, the full procedure is almost identical to the one used for generating malten, apart from the polyamine group added (Amatori S., *et al.*, 2012). Belonging to the same family of hydroxypyrones molecules derived

from maltol, maltonis shares some characteristics with malten and its derivatives. Some new variants of this compound with coordination of bivalent ions (e.g. Pd(II) or Pt(II)) are still in development, in order to find the best combination but nowadays they remain not valid alternatives to the original molecules, such as malten or maltonis.

Preliminary studies have shown the ability of maltonis to interact with DNA in *in vitro* assays through interaction between maltonis charged positive ions and DNA negatively charged. This non-covalent interaction could be the first step in the formation of the covalent cross-linking bound within chromatin structure (Amatori S., *et al.*, 2012).

First attempts to characterize the biological activity of this molecule have been done on pediatric sarcoma cells, where it has been demonstrated that maltonis reduces cell viability in monolayer tumor-growth cells in a better way than malten, while having no effect on normal mesenchymal cells (Guerzoni C. and Amatori S., *et al.*, 2014).

Maltonis was able to induce apoptosis in a dose-dependent manner and cell cycle arrest in G1 phase. In addition maltonis treatment was found to induce γ-H2AX upregulation and formation of nuclear foci, triggered by maltonis physical interaction with DNA (Guerzoni C. and Amatori S., *et al.*, 2014).

Since only the surface was scratched by these preliminary approaches to study maltonis action, the biological characteristics of maltonis have been further explored in this work.

AIM OF THE STUDY

The focus of my PhD work was centered on the characterization of the biological activity of synthetic compounds in cancer cell line models.

Previously exploration of the role of hydroxypyrone derivatives molecules has led to understanding the promising properties and roles of those compounds against cancer cells.

Some reports have evidenced the involvement of hydroxypyrones in inducing epigenetic changes when used to treat cancer cells.

In detail, one member of the hydroxypyrone family, deferiprone, has been shown to induce epigenetic changes by acting as an inhibitor of histone demethylases and increase global level of histone methylation; thus, considering the structural analogy between deferiprone and maltol, my research activity was aimed to investigate the possible epigenomic remodulation of a maltol-derived molecule, maltonis, in the NB4 cell line, considered a *bona fide* model of acute promyelocytic leukemia (APL).

MATERIALS AND METHODS

Cell culture and molecules preparation

Leukemia immortalized cell line models: acute promyelocytic leukemia (NB4), T-cell leukemia (Jurkat), acute myeloid leukemia (HL-60), chronic myelogenous leukemia (K-562), promonocytic leukemia (U937) tumor cell lines were obtained from American Type Culture Collection (ATCC) repository. Cells were grown in RPMI 1640 medium (Lonza, Belgium) supplemented with 10% FBS (Gibco, UK), 1% penicillin/streptomycin (Euroclone, Italy) and 1% L-glutamine (Lonza, Belgium). All cell lines were maintained with 5% CO_2 and a temperature of 37°C in the incubator (Fanelli M., *et al.*, 2008).

Stock solutions prepared starting from powder of maltonis and resuspended to a final concentration of 10mM in double distilled H_2O (Guerzoni C., Amatori S., *et al.*, 2014).

Stock solutions were stored at -80°C prior to use.

Treatments and cell viability evaluation

Treatments were carried out at different concentrations and time points depending on the assay. For maltonis dose response experiments were tested 0, 2, 4, 6, 8, 10, 25, 50, 100 μM in 24 hours treatment. Cellular viability was evaluated with Trypan blue dye exclusion assay by using DeNovix cell counter (DeNovix, USA). The sub-lethal dose, 10 μM maltonis, was then selected for all other experiments. For maltonis time course assay, the single dose 10 μM was tested at different time points (2, 4, 8, 16, 24 h).

Data are reported as bar plots of the mean ± standard deviation (SD) of triplicate counts.

Cell cycle analysis and hypodiploid cells estimation

NB4 cells were cultured at 1.5 x 10^5 cells/mL and treated with molecules at reported concentrations. After 24h, cells were harvested in a 15 mL falcon tube and centrifuged at 189 RCF for 3 minutes at 4°C. Then, cells were washed with 5 mL cold 1x PBS and centrifuged as before. Pellet was immediately fixed by adding 10 mL of ice-cold 70 % EtOH and samples were

stored O/N at 4°C. The day after, samples were centrifuged at 426 RCF for 3 minutes at 4°C and pellets were resuspended with 1 mL/2.5 x 10^5 cells of propidium iodide (PI) staining solution (1x PBS, 0.1% Triton X-100, PI 50 µg/mL, RNAse A 250 µg/mL). Samples were incubated covered for at least 2 hours at 4°C. Cytofluorimetric acquisition was carried out with BDAccuri C6 Plus flow cytometer (BD Life Sciences, USA). Cell cycle analyses were obtained through FlowJo software v10.8 (BD Life Sciences, USA) by using Watson-Pragmatic algorithm and results are displayed in a stacked bar plot of the mean ± standard deviation (SD) of triplicate acquisitions.

RNA extraction and sequencing

RNA was isolated starting from 2 x 10^6 NB4 cells, not treated (n.t.) and treated with 10 µM maltonis, using the RNeasy Mini Kit (QIAGEN, Germany) following the manufacturer's instructions. Purified RNA was fluorometrically quantified by Qubit RNA HS assay (Invitrogen, USA).

RNA sequencing libraries were prepared at the European Institute of Oncology (EIO, Italy), prepared according to Bonora B.M., *et al.*, 2022 and sequenced the replicates for each experimental condition (Bonora B.M., *et al.*, 2022; Amatori S., Persico G., *et al.*, 2023).

cDNA preparation and detection by real time qPCR

cDNA for NB4 n.t. and 10 µM maltonis samples were prepared using Superscript IV Reverse transcriptase (Invitrogen, USA) starting from 1 µg of RNA and following the manufacturer's instructions. Quantitative RT-PCR was performed in triplicate using 2x SYBR Green Master Mix (Roche, Switzerland), 1 µM F/R primer mix (shown in Table I), 2 µL cDNA and double-distilled H_2O to reach final volume 15 mL. Mixture reactions were amplified on the Rotor-gene 6000 robocycler (Corbett Life Science, Australia), evaluating *MYC* gene expression and normalization was carried out with housekeeping genes *GAPDH* and *ATPS.* The specificity of the PCR product was evaluated using electrophoresis agarose gel. Quantitative RT-PCR data were examined using Rotor-gene Q 2.1.0.9 (QIAGEN, Germany), to visualize and set appropriate threshold to

obtain Ct (cycle threshold). The Δ ΔCt method was used to evaluate c-MYC expression and analysis was performed using Excel.

Gene	Primer F/R
c-MYC	F -> CAGCTGCTTAGACGCTGGATT
	R -> TGGTGAAGCTAACGTTGAGGG
GAPDH	F -> CCATGTTCGTCATGGGTGTG
	R -> GGTGCTAAGCAGTTGGTGGTG
ATPS	F -> GTCTTCACAGGTCATATGGGGA
	R -> ATGGGTCCCACCATATAGAAGG

Table I. RT-PCR primer used for c-MYC analysis.

Western blotting

Hematopoietic cell lines K-562, NB4, U937, HL-60 and Jurkat were treated with 10 μM maltonis for 24h. Then, cells were resuspended in 100μL of 1x Sample Buffer (62.5 mM Tris-HCl pH 6.8, 2% SDS, 0.003% bromophenol blue, 10% glycerol, 5% β-mercaptoethanol) each 10^6 cells. A volume of 20 μL of total lysates were loaded on 10% SDS polyacrylamide gel electrophoresis and immunoblotted against the following antibodies: anti-H3K4me3 (Active Motif, 1:1000 dilution), anti-H3K9me3 (Active Motif, 1:1000 dilution), anti-H3K27ac (Abcam, 1:1000 dilution), anti-histone H3 (Sigma-Aldrich, 1:500 dilution), anti-c-MYC (Abcam, 1:1000 dilution), anti- α-Tubulin (Sigma-Aldrich, 1:500 dilution). Images were acquired using the Vü-C Imaging system (PopBio, UK).

Histone PTMs mass spectrometry analysis

Histones were enriched from 2 x 10^6 NB4 cells in triplicate for each condition as reported in Noberini R. *et al.*, 2020 and it was carried out at EIO under the supervision of the group leader Prof. Tiziana Bonaldi (Noberini R., *et al.*, 2020).

Chromatin immunoprecipitation (ChIP)

NB4 cells were treated with maltonis for 24h, then chromatin extraction and DNA isolation were performed following the procedures already described by Fanelli M., *et al.,* 2011. Isolated

chromatin was incubated in incubation buffer O/N at 4°C in a rotating platform, with following antibodies: anti-H3K4me3 (4.5 µL whole serum, Active Motif), anti-H3K27ac (0.25 µg, Abcam), anti-H3K9me3 (1.5 µL whole serum, Active Motif). Forty microliters of 50% vol/vol rec-Protein G-Sepharose 4B Conjugate (ThermoFisher, USA), preincubated 16 h at 4 °C with 1 mg/mL of BSA in incubation buffer, were added to each ChIP assay and incubated for 3 h at 4°C. After centrifugation at 2,000 RCF for 5 min at 4°C, pellets were sequentially washed with 10 mL of washing buffer A, 10 mL of washing buffer B and 10 mL of washing buffer C. Elution was carried out by incubation for 40 min at RT, using a rotating platform, in 300 µL of elution buffer. After centrifugation (1,270 RCF for 2 min at 4°C), the supernatant was recovered and repeated the step with only 50 µL of elution buffer as described above (vortexing 10 s at maximum speed before centrifuge) to obtain a final volume of 0.35 mL (named “bound” fraction).

DNA isolation and locus-specific analysis by real-time qPCR

Bound fractions and an amount corresponding to 5% of chromatin used to IP (input), were de-crosslinked through an O/N incubation at 65 °C with 0.2 M NaCl, followed by digestion with 0.1 mg/mL proteinase K (3 h at 45°C). DNA purification was carried out using the PCR Purification Kit (Qiagen, Germany) following manufacturer’s instructions and DNA was fluorometrically quantified by Qubit (Invitrogen, USA) using the dsDNA HS Assay Kit (Invitrogen, USA). The specificity of the immunoselection was preliminarily analyzed by real-time quantitative PCR (qPCR) using the Fast Start SYBR Green Master Mix (Roche, Switzerland) and a set of primers pairs specific for known positive (enriched) and negative (not enriched) control regions (Table II) as previously described (Amatori S., *et al.,* 2014).

Gene	Primer F/R
hVCL	F: ATGCCAGTGTTTCATACGCG R: CGCCCTCCTCGTGCATTAT
hCol2a	F: CGCAACGTAGGGACCTGCA R: CGCCGACTTAGGCACAGGAC
hGAPDH	F: GCAAATTCCATGGCACCGT R: TCGCCCCACTTGATTTTGG
Sat2	F: CGAATGGAATCGAATGGAAT R: ATTCCATTCGATTCCATTCG
Alpha Sat	F: AGCTGAATTCTCAGTAACTTCCTTGTGTTGTGT R: AGCTGAATCATTCTGACTAGTTTCTATAGG

Table II. Primer pairs used to analyze purified DNA immunoselected by ChIP-seq. The hVCL primer pair was used as positive control, while hCol2a primer pair as negative control.

Amplifications of bound and input fractions were carried out using the Rotor-Gene 6000 robocycler (Corbett Life Science, Australia) and analyzed using the $2^{-\Delta\Delta Ct}$ method to estimate the enrichment against input.

Library preparation, sequencing and bioinformatic analysis

Library preparation and sequencing were performed at the NGS facility in EIO as reported in Amatori S., Persico G., *et al.*, 2023 under the supervision of PhD Giuseppe Persico, who also performed RNA-seq and ChIP-seq bioinformatic analysis. Peaks were visualized using Integrative Genome Viewer (IGV) from where snapshots were produced (Amatori S., Persico G., *et al.*, 2023).

Histone K9 methyltransferases inhibition assay

NB4 cells were plated at 2 x 10^5 cells/mL and treated with 100 μM maltonis for 24 hours. Cells were harvested in 15mL tube and nuclear extraction was performed according to manufacturers' instructions (Epiquik Nuclear Extraction Kit I; Epigentek Inc., USA), followed by quantification of the protein amount with Qubit protein assay (Invitrogen, USA). Thus, nuclear extracts were processed with the histone methyltransferase inhibition assay according to manufacturers' instructions (Epiquik Histone methyltransferase activity/inhibition assay kit (H3-K9); Epigentek

Inc., USA). The measurement of different OD450nm was obtained with a microplate reader (Bio-Rad, USA) and results were reported in a bar plot of the mean ± SD values from the tripled experiments.

In silico analysis of correlation between maltonis effect and *MYC* expression

A correlation analysis was evaluated between grouped NCI 60 cancer cell lines based on mRNA z-score *MYC* expression (CBioportal, https://www.cbioportal.org/) dataset for NCI60 cell lines, and maltonis effect (previously obtained from NCI 60 screening). Representative box plot analysis of grouped cancer cell lines based on mRNA z-score *MYC* expression and maltonis effect was built as: high responsive group, consisting of blood and colorectal cancer cells; less responsive group, consisting of all other cells. Statistical significance was performed using a t-student test (comparison of means) between the two groups of cells, p-value < 0.0001.

Statistical analysis

Statistical analyses and plots were generated using MedCalc for Windows, version 19.4 (MedCalc Software, Belgium), R or GraphPad Prism 9.51 for all experiments reported in the results section.

RESULTS

1. ANTIPROLIFERATIVE ACTIVITY OF MALTONIS

A preliminary drug screening of the molecule for its efficacy was made by submission of maltonis to the National Cancer Institute (NCI) in the USA, to be included in the NCI-60 Human Tumor Cell Lines Screen.

The submitted compound, as approved in early 2007, was tested in 60 cell lines in a one dose screen (10 μM) and the growth assay was relative to no-drug control, allowing the determination of both growth inhibition (GI) and lethality values in 48h of treatment. The cell lines screened by NCI-60 are divided per tumor category: leukemia, melanoma, colon, breast, brain, renal, lung, ovarian, prostate and kidney cancer, with the final goal to help discover new compounds to inhibit tumor cell growth (Shoemaker R., 2006). All cancer cell lines are grown in RPMI1640 medium containing 5% of FBS and 2mM of L-glutamine.

Maltonis has shown potential antineoplastic activity towards different tumor cell lines, more specifically against the groups of leukemia and colon cancer cells (Figure 1).

Considering the obtained result and the similarity of maltonis with deferiprone, another hydroxypyrone member that as shown potential antiproliferative activity in cancer cell lines and it acts through an epigenetic mechanism, it was chosen to investigate the activity of the molecule in the NB4 cell line as a model of APL. This tumor type is characterized by the presence of the fusion gene PML/RARα, which exerts its activity through recruitment of repressive complexes to target gene promoters, and by epigenetic perturbations (e.g., H3K9me3) (Mehdipour P., *et al.*, 2015). NB4 cells were tested in the same conditions in our laboratory, showing to be the most sensitive cell line among leukemia cells (Figure 1).

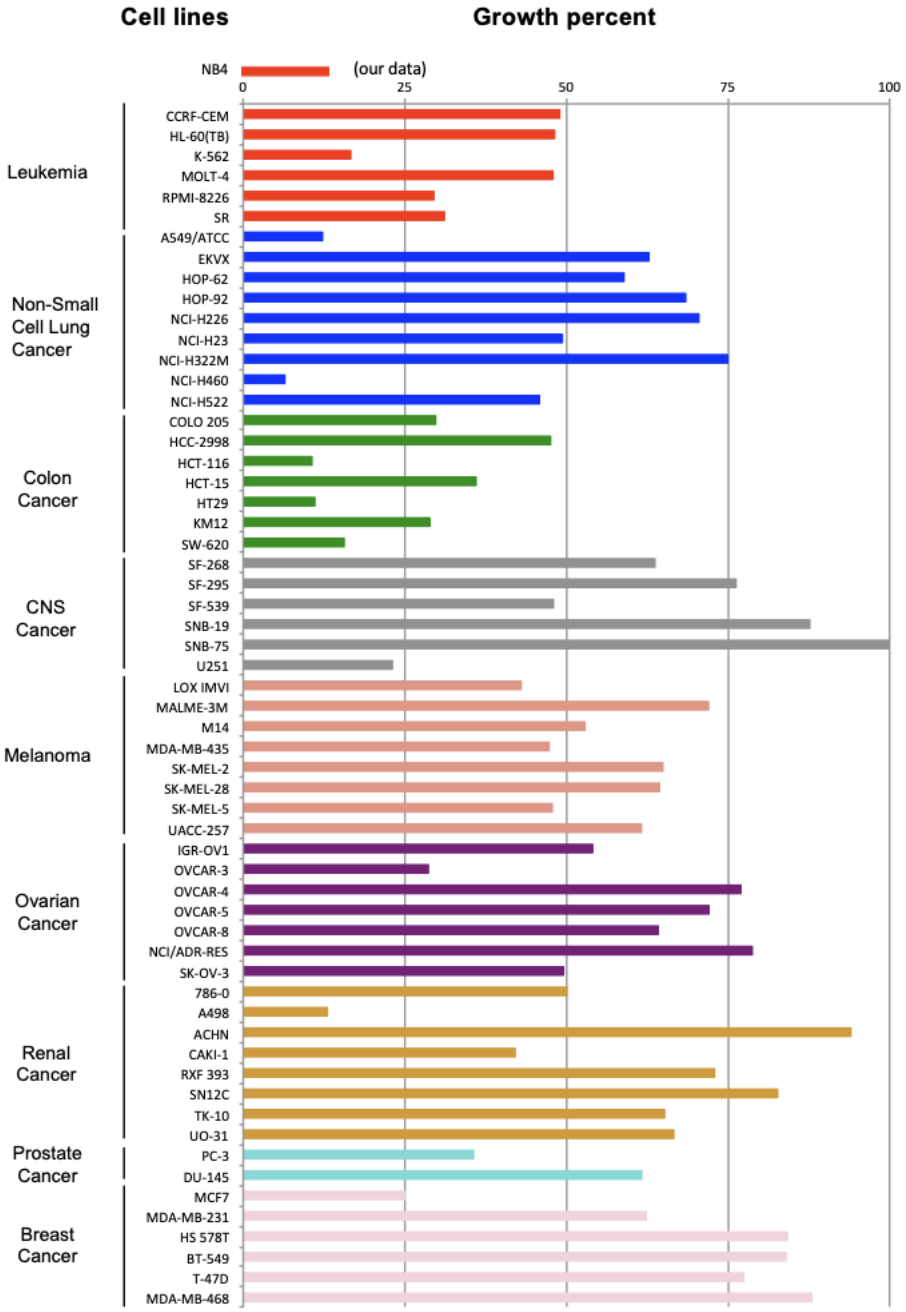

Figure 1. NCI60 screening of 48h single dose maltonis treatment. Bar plot of growth percentage for NCI-60 panel of 59 human tumor cell lines, divided per tumor type, screened with maltonis by the developmental therapeutics program (DTP) from National Institute of Cancer (NCI/NIH). Cells were incubated with maltonis 10 μM for 48 hours and growth percentage was evaluated as ratio between treated/untreated cells. NB4 cells were tested in our laboratory and growth percentage was added above the graphical representation.

1.1 Effect of maltonis 24 hours treatment in APL NB4 cells

NB4 APL cells were exposed to maltonis for 24 hours, in a dose response experiment ranging from 2 μM to 100 μM.

It was observed a dose-dependent decrease of cell survival in 24 hours, with higher doses showing the most dramatic rate of survival (Figure 2).

In the light of the results obtained, the sub-lethal dose of 10 μM treatment was selected as the experimental condition to be used in other analyses, with a survival rate of 78 %.

In addition, other hematopoietic cancer cells have been tested at designed dose, among which were Jurkat, HL-60, K-562 and U937, resulting in a similar cell survival rate to NB4 cells and confirming the previously discussed result obtained by NCI-60 screening (Table 1).

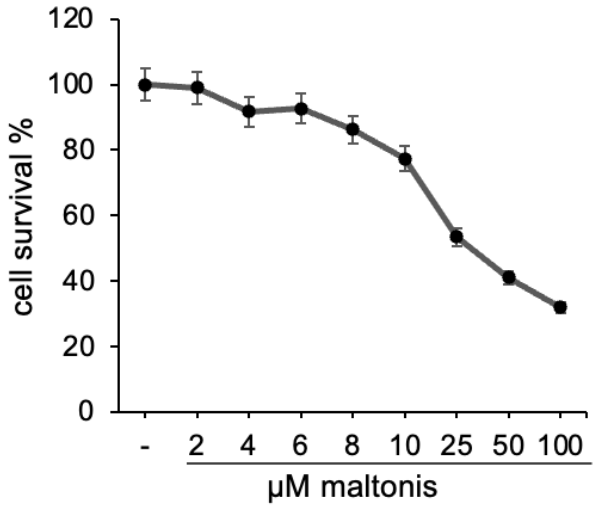

Figure 2. Dose response treatment in 24h of NB4 cells. Dose response assay where NB4 cells were treated for 24 hours with or without maltonis at reported concentrations. Data reported as mean value ± standard deviation (SD) of a three experimental replicate.

cell lines	μM	mean living cells	cell survival
HL-60	-	3.10 ± 0.23 x10⁵ cells/mL	100 %
	10	2.16 ± 0.36 x10⁵ cells/mL	70 %
K562	-	3.40 ± 0.58 x10⁵ cells/mL	100 %
	10	2.34 ± 0.32 x10⁵ cells/mL	69 %
Jurkat	-	3.75 ± 0.23 x10⁵ cells/mL	100 %
	10	2.98 ± 0.18 x10⁵ cells/mL	79 %
U937	-	4.00 ± 0.54 x10⁵ cells/mL	100 %
	10	3.11 ± 0.38 x10⁵ cells/mL	78 %

Table 1. Leukemia cells (HL-60, Jurkat, K562, U937) untreated (n.t.) and treated (maltonis) with a 10 μM dose of the compound for 24 hours.

1.2 Maltonis induce cell cycle alteration in NB4 cells

The biological activity of maltonis in NB4 cells was then monitored through cell cycle analysis. The chosen cellular model was treated with the molecule for 24 hours in a dose response experiment ranging from 2 μM to 10 μM (Figure 3). It was found that maltonis induces important cell cycle alterations, with an accumulation of cells in G2-M phase starting from 6 μM dose (Figure 3).

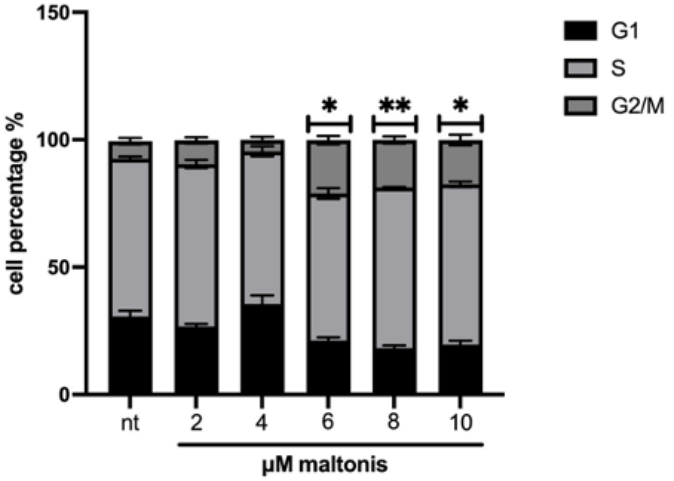

Figure 3. NB4 cells cell cycle analysis after 24 h treatment with maltonis. NB4 cells cycle analysis of 24 hours dose response with maltonis at reported concentrations. Data are shown as mean value ± SD of three replicates and asterisks indicate the significancy of G2 phase relative to not treated (n.t.) sample evaluated by student t-test (* = $p < 0.05$; ** = $p < 0.01$).

Moreover, I have evaluated the ability of the compound to induce cell-death by monitoring hypodiploid cells' percentage at sub-G_0, where they are clearly accumulating in a dose dependent manner (Figure 4). This result was in accordance with previously reported data where maltonis was able to induce tumor cells death and trigger apoptosis response in sarcoma cells (Guerzoni C., Amatori S., *et al.*, 2014).

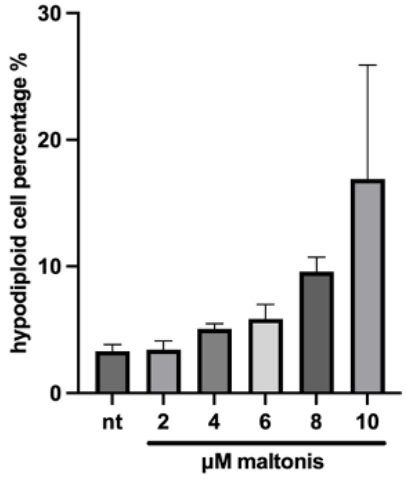

Figure 4. Hypodiploidy analysis in NB4 cells dose response treatment with maltonis for 24 h. Hypodiploidy cell percentage evaluated in 24 hours at reported doses of maltonis. Hypodiploidy percentage was evaluated by analyzing flow cytometry raw data obtained with propidium iodide staining. Data reported as mean of three replicates ± SD.

Then, I have also checked the effect of treatment on cell cycle through time, treating NB4 cells with a single-dose of maltonis (10 μM) and collecting cells at 8, 16, 24 hours (Figure 5).

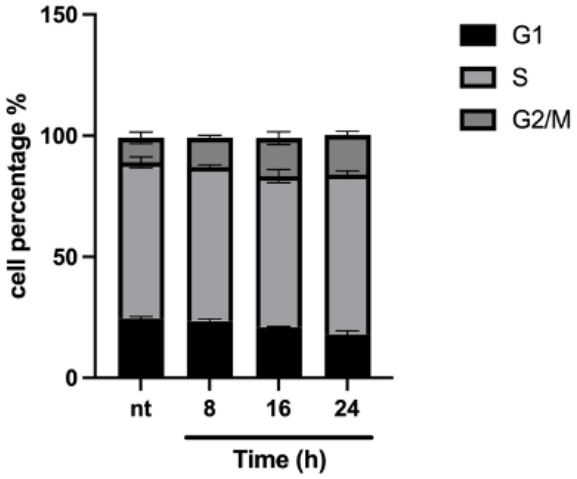

Figure 5. Timecourse evaluation of cell cycle in NB4 cells treated with maltonis. Barplot representing the timecourse (8, 16, 24 hours) evaluation of cell cycle phases during one dose (10 μM) maltonis treatment in NB4 cells. Data are reported as mean ± SD

2. MODULATION OF GENE EXPRESSION PROFILE IN NB4 CELLS

To define the biological response of maltonis, I have analyzed the gene expression profile of the NB4 cells. The experiment was performed in three biological replicates of not treated and treated cells with 10 μM of maltonis for 24 hours where, after RNAs extraction, they were sequenced and analyzed.

For the analysis, after removing the low expressed genes (25 % genes value with low RPMK), the remaining number of genes were 17989 and they were used to select the most variable 10 % of them to further characterize their relationship through hierarchical and PCA analysis (Figure 6).

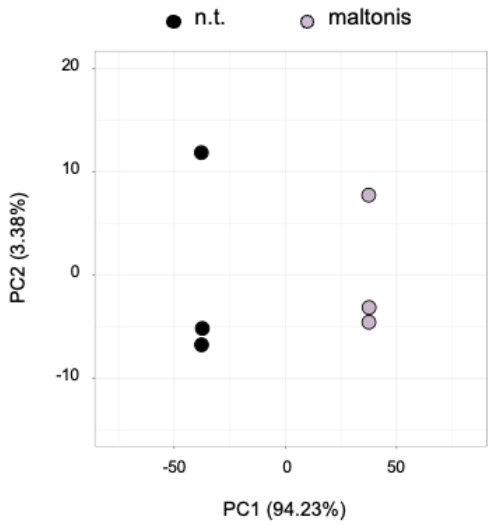

Figure 6. PCA plot. Principal component analysis (PCA) of untreated (n.t., black dots) and maltonis (10 μM, lilac dots) of normalized RNA-seq data three replicates for each condition. PC1 and PC2 values are reported in graph.

The PCA plot evidenced the clear clusterization in distinct profiles between maltonis treated and untreated samples, where the first principal component PC1 is 94.23 % and the second principal component PC2 is 3.38 %, explaining the total variability of our dataset. This allows us to speculate about the profound modulation of gene expression that maltonis treatment induces on NB4 cells.

Differential gene expression was performed with the edgeR package, filtering 551 genes downregulated and 288 upregulated genes as the most significantly affected by the treatment

(Figure 7A). The obtained gene list was then used for the gene set enrichment analysis (GSEA), to evaluate gene pathways affected by maltonis treatment. GSEA analysis revealed an interesting upregulation of interferon-like pathways, with a normalization enriched score (NES) of +2.40 and +1.95, and downregulation of genes related to c-MYC pathways, with a NES of -2.53 and -2.41 (Figure 7B).

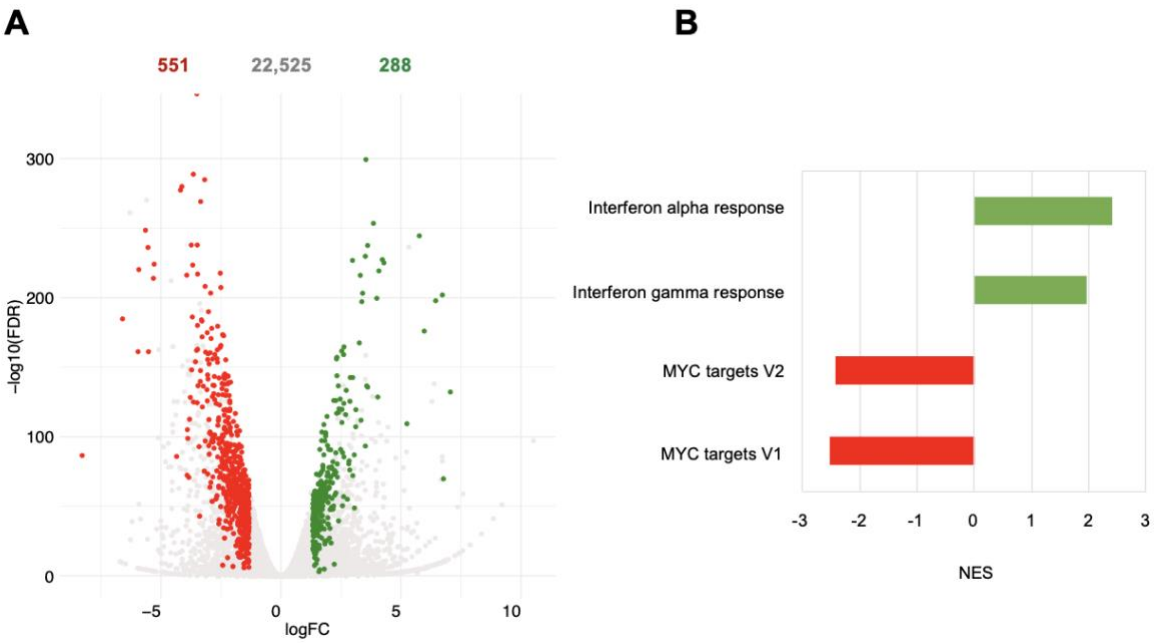

Figure 7. Volcano Plot and GSEA analysis. A) Volcano plot of RNA-seq normalized data. Data shows differential expressed genes (DEGs), following these restrictions: FC ≥ ± 2.5; FDR ≤ 0.01; RPKM (reads per kilobase per transcript per million) > 10K. Green dots represent upregulated transcripts, while red dots indicate downregulated genes. The total number of genes analyzed and the upregulated/downregulated number were reported in graph. **B)** Gene set enrichment analysis (GSEA) evidenced the most significant, through normalized expression significance (NES), pathways upregulated (green) and downregulated (red) by maltonis in 24 hours.

3. EPIGENOMIC REMODULATION CAUSED BY MALTONIS IN NB4 CELLS

Previous studies and our recently published article have explored the potential mechanism of action of maltonis, specifically its ability to interact with DNA structure and induce cross-linking events within stable and structured chromatin (Guerzoni C., Amatori S., *et al.*, 2014; Amatori S., Persico G., *et al.*, 2023). Based on this mode of action and the previously observed in Guerzoni C., Amatori S., *et al.*, 2014 increase in γH2A-X expression resulting from double-strand breaks, it was investigated the hypothesis that maltonis could remodel the epigenomic profile of NB4 cells. A particular focus was posed on the redistribution of the H3K9me3 mark since, as highlighted by Ayrapetov M.K. *et al.* in 2014, indeed this mark is redistributed upon γH2A-X recruitment at damage sites.

3.1 Global epigenetic change of lysine 9 methylation

Following the aforementioned hypothesis, global lysine 9 methylation levels were investigated. Firstly, it was assessed the protein levels through a Western Blot assay. NB4 cells were cultured for 24 hours with or without different concentrations of maltonis (10 μM, 50 μM, and 100 μM), and total lysates were prepared. The immunoblot analysis demonstrated a dose-dependent reduction in the H3K9me3 mark globally, confirming the hypothesis mentioned previously (Figure 8A).

To further evaluate this global reduction, it was used the Epigentek Inhibition of K9 methyltransferases assay kit. NB4 cells were cultured for 24 hours, both untreated and treated with 100 μM maltonis, the highest dose used in WB to better look at the phenomenon. Subsequently, it was followed the instructions provided by the manufacturer to isolate nuclear lysates and perform the inhibition of K9 methyltransferases.

The analysis revealed a significant reduction (ρ value < 0.05) in methyltransferase activity at tested dose after 24 hours (64.01 %) (Figure 8B). This finding could suggest that the observed global reduction of the histone mark at different maltonis concentrations, observed in WB, may

be associated also at lower doses with a corresponding decrease in the protein expression levels of epigenetic writers involved in the H3K9 methylation mark.

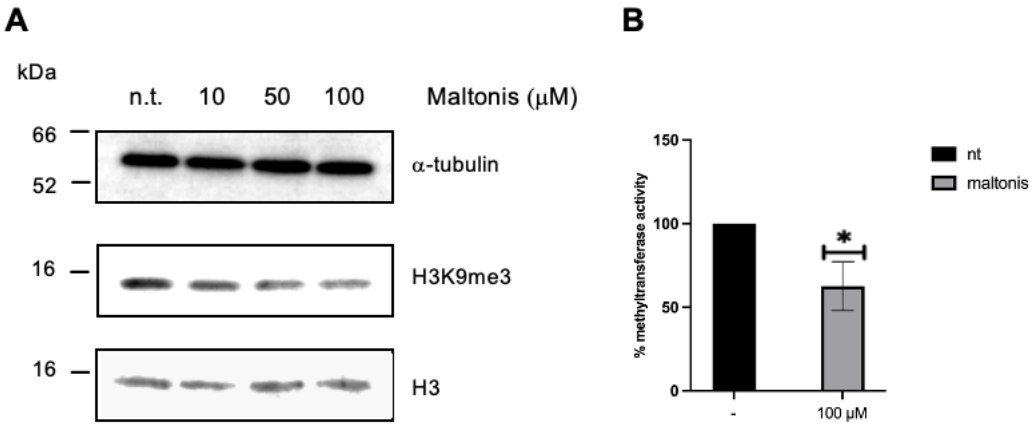

Figure 8. Global evaluation of H3 lysine 9 methylation. A) Western Blot evaluation of the H3K9me3 mark induced by maltonis at different reported concentrations. **B)** Evaluation of lysine 9 methyltransferases activity after 24 hours treatment with maltonis. Data reported as mean value ± SD of three independent experiments and asterisk indicates the significancy relative to not treated (n.t.) sample evaluated by student t-test (* = $p < 0.05$).

3.2 Maltonis remodels the epigenome

The possibility that maltonis could induce a remodulation of the epigenome, drove to analyze global HPTMs levels by mass spectrometry in NB4 cells untreated and treated (10 μM) for 24 hours. The result obtained was a massive rearrangement of HPTMs, such as H3K27ac, H3K27me1 and H3K4me3 upregulation while global acetylation on histone H4, H3K79 methylation, H3K36me2 and H3K14ac were downregulated by the treatment (Figure 9A). Subsequently, the attention was focused on the well-studied marks associated with transcriptional activation H3K4me3 and H3K27ac, while H3K9me3 for the transcriptional repression. As shown in figure 9B, the scatter plot for the triplicates samples of the three investigated HPTMs, reveal a significant difference between untreated and treated samples and underly the global remodulation that NB4 cells undergo upon maltonis treatment.

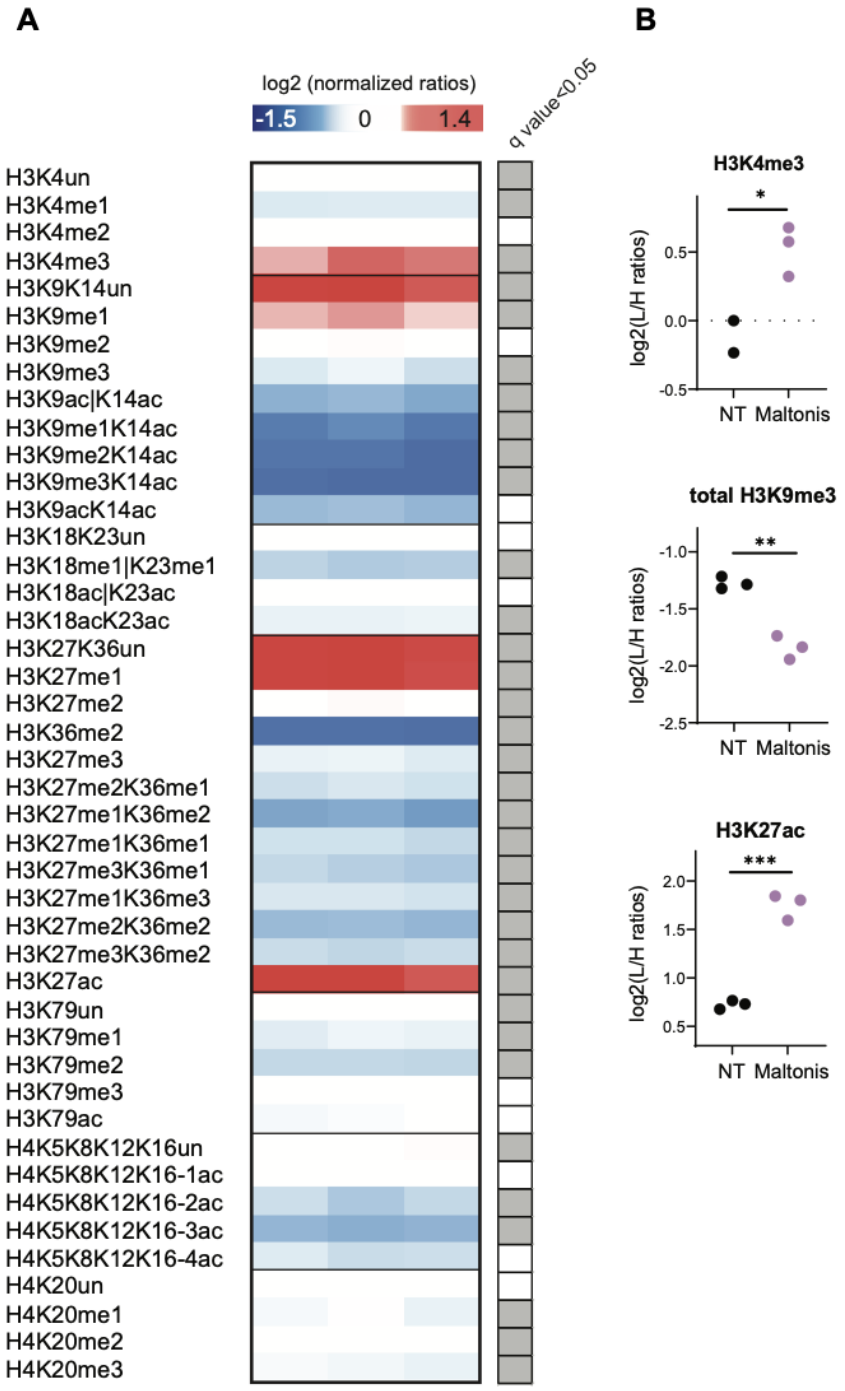

Figure 9. Mass-spectrometry evaluation of NB4 cells HPTMs. A) Heatmap of different histone post-translational modifications (HPTMs) in NB4 cells treated with 10 μM of maltonis. Data obtained as ratio of light/heavy (L/H) peptides relative abundances normalized with L/H of untreated sample. **B)** Scatter plot displaying L/H ratios for untreated and treated samples of the three histone marks object of the study. Total H3K9me3 indicates the sum of all peptides containing K9me3.

3.3 Genome-wide re-distribution of HPTMs and comparison between ChIP-seq and RNA-seq expression

The three modifications selected to be investigated, H3K9me3, H3K4me3 and H3K27ac, were processed through ChIP-seq following the methodology outlined in Amatori *et al.*, 2018. The experimental conditions were the same already described in the previous paragraphs.

Initially, a PCA plot was generated to assess the clustering patterns of the samples based on the two principal components, from which it is evident that each histone modification occupies a distinct cluster (Figure 10). Moreover, each histone post-translational modification (HPTM) exhibited noticeable separation based on the treatment, with more pronounced differences observed for H3K27ac and H3K9me3.

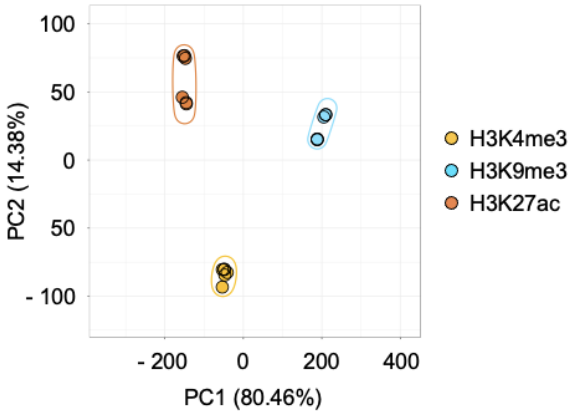

Figure 10. PCA plot of ChIP-seq histone marks. PCA plot showing clustering of H3K4me3, H3K9me3 and H3K27ac ChIP-seq for untreated and treated samples.

Differential enrichment analysis performed through the DiffBind package in R has been used for defining enriched or depleted regions associated with the HPTMs under investigation. Subsequently, annotation of the regions was performed using the ChIPSeeker package. The findings of the study reveal that:

1. in H3K4me3 the total number of differential expressed regions (DERs) were n = 3,353, where 1,187 were enriched regions and 2,166 the depleted DERs. Interestingly for this mark, the half majority (60 %) of DERs in depleted regions were found in promoter regions, instead of the only 38 % found in enriched ones;

2. in H3K27ac the total number of DERs corresponded to n = 6,586, where 2,381 DERs enriched and 4,205 depleted. This mark has shown an opposite behavior compared to other transcriptional activation mark H3K4me3, presenting the 43 % of DERs in the promoter region of enriched regions and only 25 % in depleted DERs;

3. in H3K9me3 the total number of DERs were n = 839, with enriched DERs n = 717 and depleted n = 122. The repressive mark has shown to be enriched in promoter regions in 59 % of DERs, while the most interesting DERs depleted were the distal regions within 54 % of total depleted DERs (Figure 11).

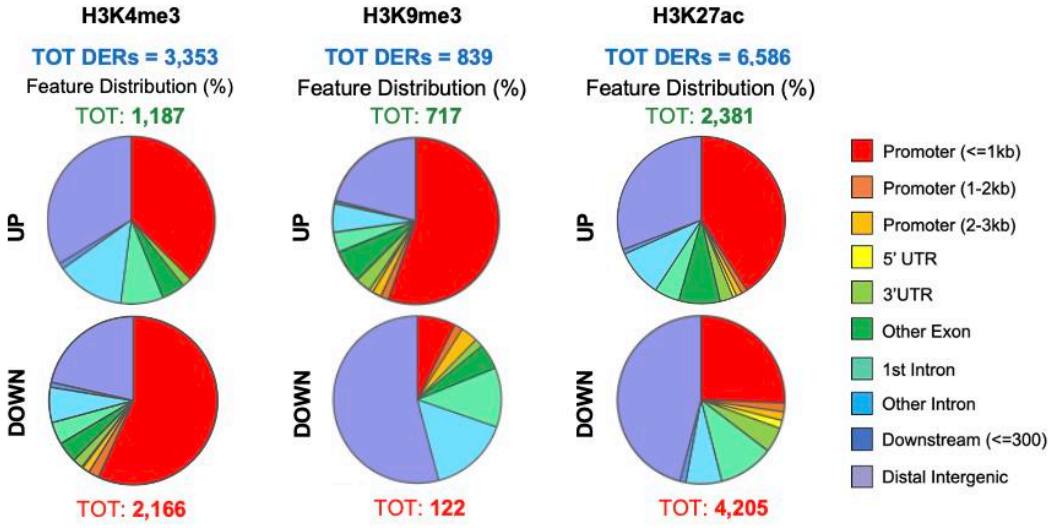

Figure 11. Genomic distribution of histone marks upon maltonis treatment. Graphical representation of genomic distribution of HPTMs investigated. The pie charts show the number of total DERs annotated after maltonis treatment. Total DERs enriched (UP) are in green and depleted (DOWN) in red.

Consequently, a comparative analysis of gene expression data from RNA-seq with the epigenomic data was conducted to gain insight into the potential association of the redistribution of histone marks and the expression profile. As expected, it was found a strong association between the two transcriptional activation marks and related transcripts. Specifically, genes associated with promoter region enrichment of those marks were also upregulated in RNA-seq and genes with DERs depletion in promoters identified also in decreased expression transcripts (Figure 12A). However, there was no significant correlation between ChIP-seq data and RNA-

seq data for H3K9me3, suggesting that the global reduction of this modification was not linked to gene expression and required other investigations.

To gain further insights into the biological significance of genes associated with the histone post-translational modifications (HPTMs) and RNA-seq data, a Gene Set Enrichment Analysis (GSEA) was managed. These findings confirmed that the gene expression pathways identified earlier and discussed above are in alignment with the epigenomic data. Specifically, both H3K4me3 and H3K27ac shared with the RNA dataset the upregulation of interferon alpha and gamma pathways and the downregulation of IL-2/STAT5, WNT beta catenin and KRAS signaling (KRAS-Upregulated genes) pathways (Figure 12B). Furthermore, H3K4me3 alone confirmed the downregulation of c-MYC observed in gene expression. On the other hand, H3K27ac was associated with the upregulation of DNA repair genes, unfolded protein and E2F upregulated targets, as well as the downregulation of pathways related to epithelial-mesenchymal transition and TGF-beta signaling. Interestingly, H3K9me3 analysis exhibited only a downregulation of the interferon alpha response gene set, which was upregulated on the contrary in other modifications (Figure 12B). This once again highlights the undefined role of the mark in accordance with previous analysis.

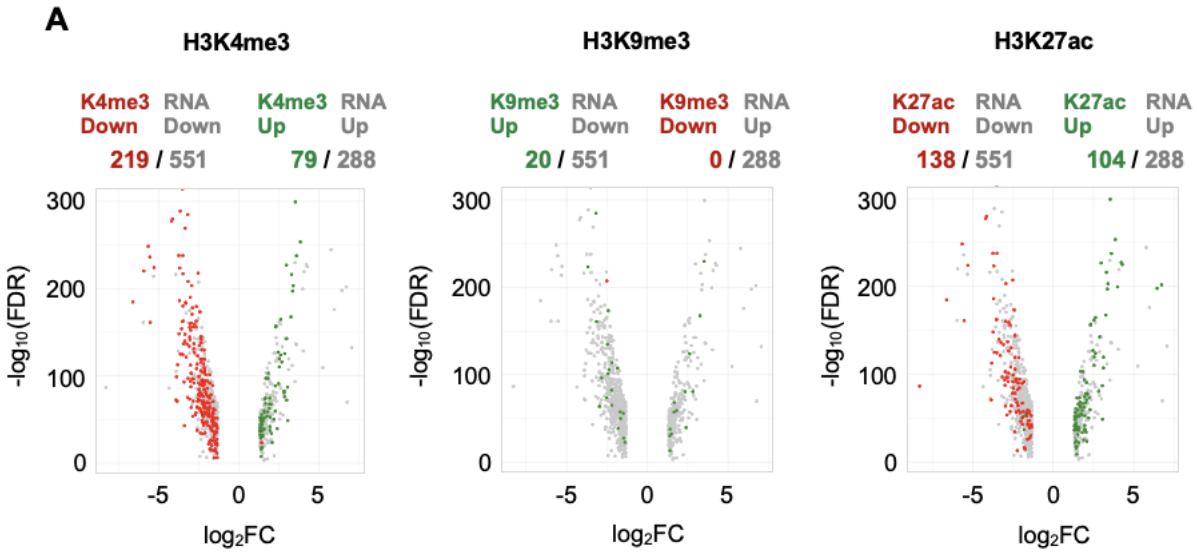

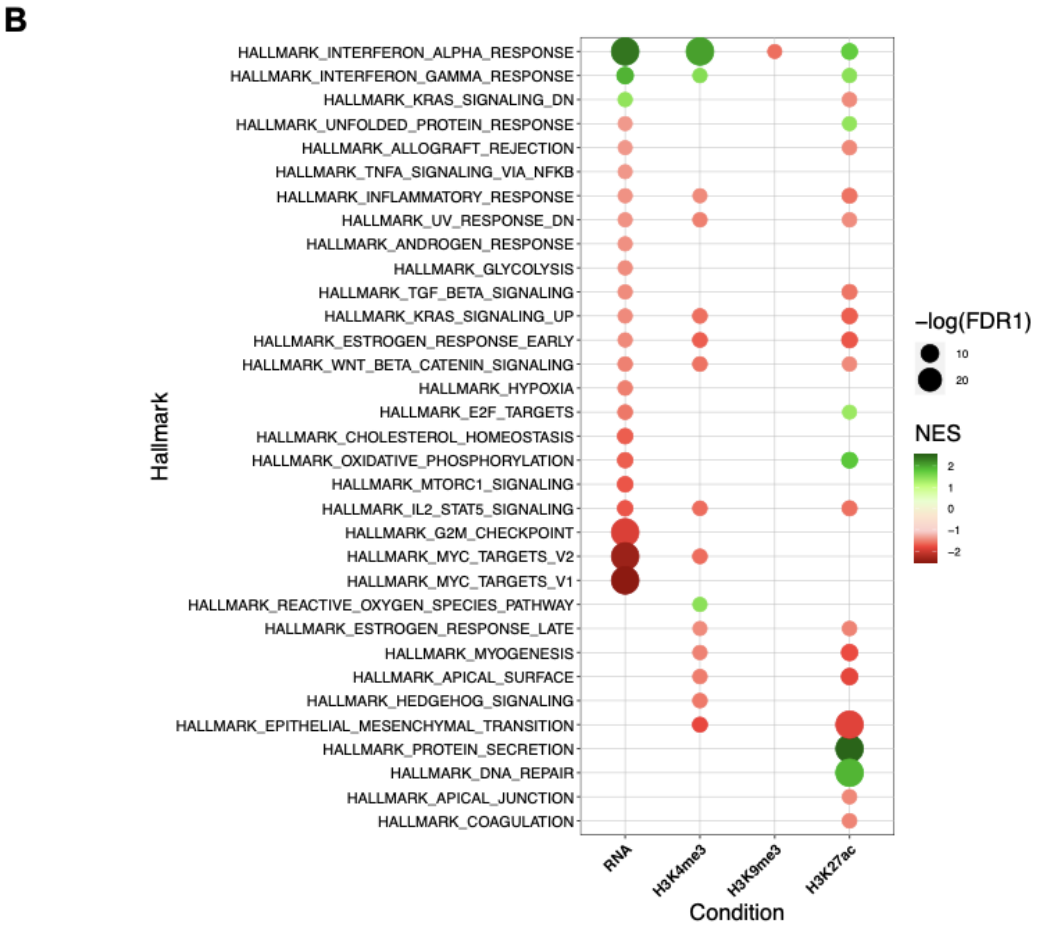

Figure 12. Comparative analysis of RNA and ChIP-seq data. A) Volcano plot of DEGs for the three different epigenetic marks under investigation. DEGs enriched or depleted of HPTM are evidenced in green or red respectively, while in grey it is reported the number of DEGs not epigenetically modified. Number of genes epigenetically regulated are reported in graph. **B)** GSEA analysis of DEGs evidence the hallmarks colored in green or red depending on the NES. The dimension of dots reflects the FDR as reported in the legend in graph.

3.4 H3K9me3 is evicted from pericentromeric regions and transposable elements

To address the question related to H3K9me3 global downregulation, it was observed the genomic distribution of this mark resulted from annotation analysis. As highlighted in the previous paragraph, H3K9me3 is mainly found at distal intergenic regions. This epigenetic mark is mainly associated with heterochromatin and cell fate, so the observed distribution shown at distal intergenic regions is not surprising (Becker J.S., Nicetto D., Zaret K.S., 2015).

To further characterize the global reduction resulted from the treatment with maltonis, I have decided to investigate the possible variation at pericentromeric and centromeric chromosomal regions, which are well known to be enriched in heterochromatin, where also H3K9me3 is embedded (Montavon T., *et al.*, 2021). To study those regions, it was analyzed the DNA purified from chromatin immunoselected with antibody against H3K9me3 for not treated and treated (10, 50, 100 μM) samples by quantitative RT-PCR using primer pairs for alpha satellite and satellite-2 DNA regions (Table 2, Materials and methods). The experiment was conducted in triplicate and the data show that the relative amount of H3K9me3 abundance at those regions is reduced significantly in a dose dependent manner (Figure 14).

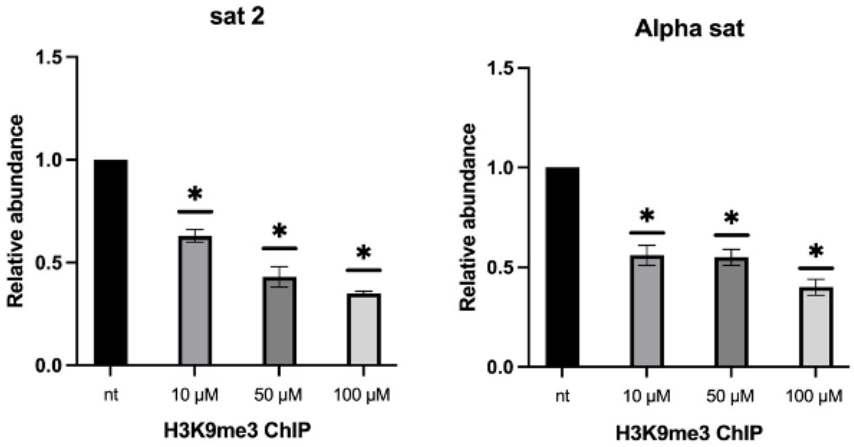

Figure 14. Pericentromeric and centromeric DNA regions analyzed through RT-PCR of H3K9me3 ChIP-seq. Bar plot of relative abundance of H3K9me3 at satellite 2 (right) and Alpha satellite (left) DNA regions evaluated through RT-PCR on DNA purified immunoselected for H3K9me3 mark. Significancy was calculated with a student t-test (two-sided), p value < 0.02.

Based on these findings and to further date the hypothesis of the major contribution of constitutive heterochromatin enriched in repetitive DNA regions to H3K9me3 depletion, the consequences of this reduction have been investigated in terms of release of transposable elements (TEs), which are described in literature to be transcriptionally silenced and enriched of H3K9me3; they are also embedded everywhere in the genome, primarily in those heterochromatin repetitive regions (Wood G.J. and Helfand S.J., 2013; Marsano R.M. and Dimitri P., 2022). Thus, using the TEtranscript package for differential expression analysis of

transposable elements in RNA-seq datasets, a total n = 390 TE families have been identified, with 91.8 % of TE upregulated compared to only 8.2 % being downregulated (Figure 15A). Furthermore, by examining the replicates of untreated and treated samples, it was observed that the H3K9me3 signal was lower across LTRs compared to the untreated samples (Figure 15B) and that these TEs were the most differential expressed after treatment (Table 2). This finding reinforces the relationship between the loss of the H3K9me3 mark at heterochromatin enriched regions and the upregulation of these repetitive elements. Understanding the role of H3K9me3 in maltonis treatment is crucial, as it may provide insights into the activation of genes associated with the inflammatory response.

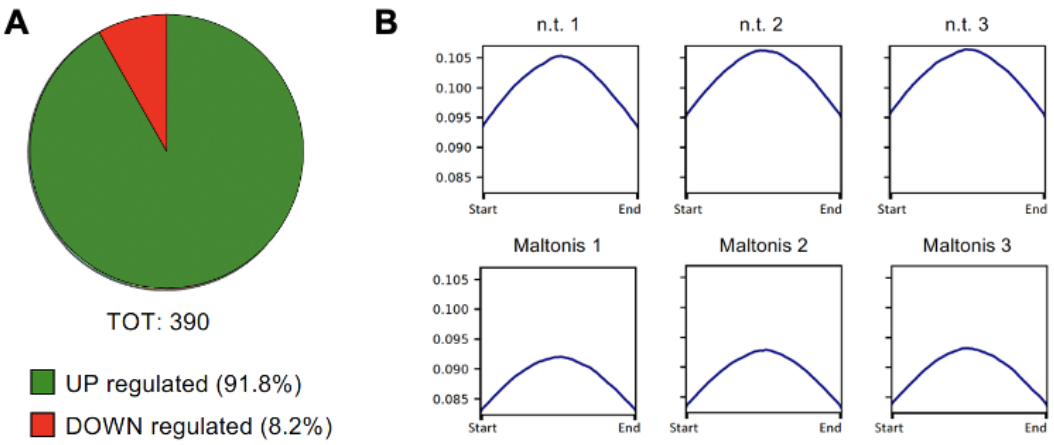

Figure 15. Transposable elements upregulation upon maltonis treatment. A) graphical representation of TEs percentages of upregulated and downregulated families. **B)** The figure represents the H3K9me3 deposition at LTRs sites in normal condition (n.t.) and treated (maltonis) for each biological replicates.

TEs	n°
LTR	271
SINE	29
LINE	24
Satellite	8
DNA	44
Unknown	6
Other	6
Helitron	1

Table 2. List of TE elements. TE elements analyzed through TEtranscript using DEseq2 package, uncovering among differential expressed TEs a total of 390 elements, where the major contribution is given by LTR (=291).

4. c-MYC IS MASTER REGULATOR OF DOWNREGULATED GENES

Conspicuously, as shown in paragraph 2, with the gene expression pathways remodulation induced by maltonis treatment, there was the massive downregulation of target genes associated with c-MYC.

The downregulated pathways identified through GSEA had a common feature: the involvement of c-MYC as a master regulator of the associated genes. This is demonstrated in the Venn diagram (Figure 16), which highlights the main pathways that contributed to the normalized enrichment score (NES) and shared c-MYC as the main regulator as: MYC targets V1 and V2 (a group of c-MYC target genes, including those associated with proliferation), the G2M checkpoint pathway and the IL2/STAT5 signaling pathway.

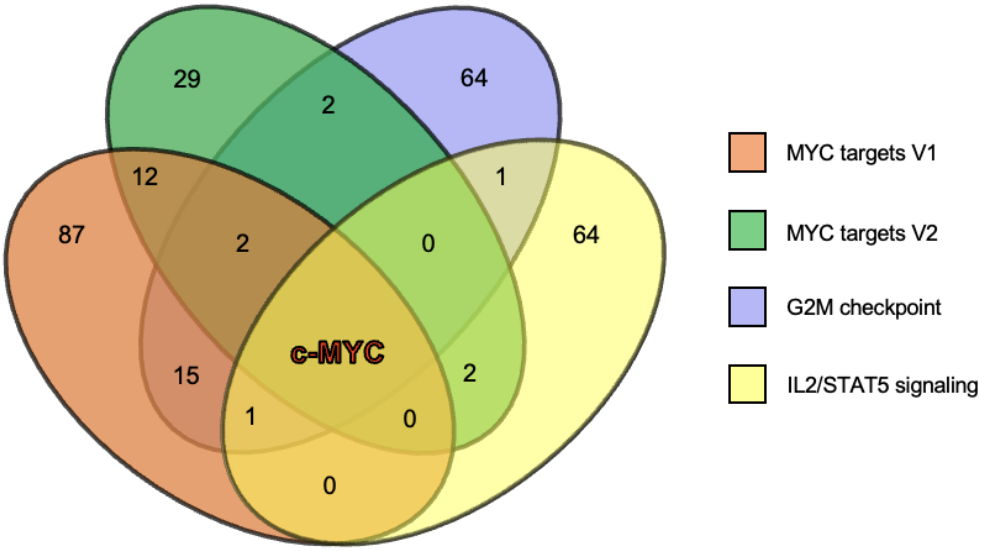

Figure 16. Venn diagram of master regulator c-MYC. c-MYC is depicted as the master regulator of all the downregulated genes, as it is the core center of principal pathways resulting downregulated by maltonis.

4.1 *In silico* evaluation of c-Myc expression and maltonis effect

In order to further understand the role of c-MYC expression resulting in our cellular model, the NB4 APL cell line, an *in silico* analysis was assessed to evaluate the mRNA expression of c-MYC among maltonis biological response of NCI-60 cell lines.

First, it was obtained the mRNA z-score from c-Bioportal dataset for NCI-60 cell lines and the maltonis effect on those cells from the NCI-60 data.

As shown in figure 17A, in the multitude of cancer cell groups, the two cancer types that present the most abundant c-MYC mRNA expression were: blood cancers (z-score mean 1.41) and colorectal cancer (z-score mean 0.57), noting that the majority of other z-score mean values for the remaining cancer types are below zero and that the two cancer types having the higher mRNA z-score are the most sensitive to treatment. The same analysis was repeated with the Cellminer dataset with fragment per kilobase per million reads (FPKM) for c-MYC expression. Again, the trend monitored is the same as the one obtained with cBioportal dataset.

Additionally, the division of cancer groups in two categories, high responsive groups and low responsive groups, showed a better view on the different expression of c-MYC in cancer cell types that are most sensitive to maltonis treatment (Figure 17B). Therefore, this result suggested an evident correlation between c-MYC expression and maltonis effect, probably dependent on cell duplication. Since several evidences indicate the importance of targeting c-MYC to overcome drug resistance and regain sensitivity to treatment and thus, its downregulation was investigated in the NB4 cell model (Pan X.N., *et al.*, 2014; Strippoli A., *et al.*, 2020).

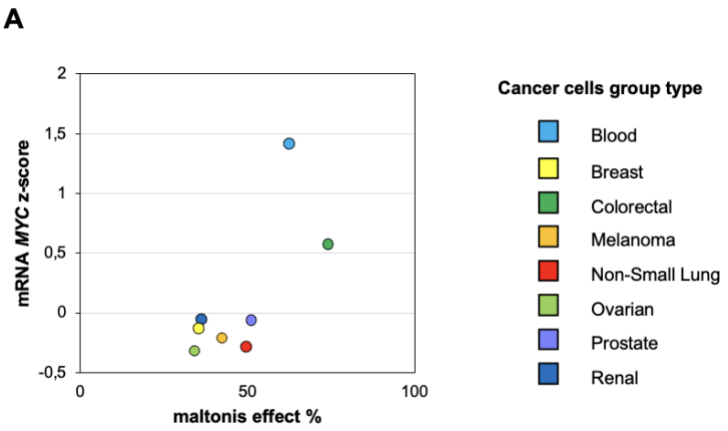

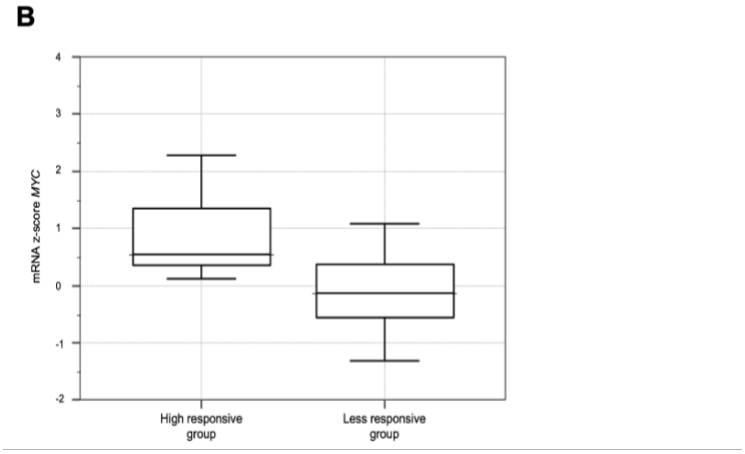

Figure 17. *In silico* analysis of maltonis effect and c-Myc expression. A) Scatter plot of grouped NCI 60 cancer cell lines based on mRNA z-score *MYC* expression, through CBioportal dataset for NCI60 cell lines, and maltonis effect obtained through NCI60 panel data. **B)** Representative boxplot analysis of grouped cancer cell lines based on mRNA z-score *MYC* expression and maltonis effect (high responsive group: blood and colorectal cancer cells; less responsive group: other cells, reported in legend). For each box, median is represented within a line across the box. Statistical significancy was performed using a t-student test (comparison of means) between the two group of cells, p value < 0.0001.

4.2 c-Myc is downregulated at both transcriptional and protein level

The gene expression analysis has revealed a central role for c-MYC in maltonis treatment response by NB4 cells. Indeed, the *MYC* transcript expression is decreased (-3.6 folds) upon 24 hours of treatment with maltonis. Afterwards, it was checked if the histone modifications studied were associated with this lowered expression of the transcript. It was observed that, aside from H3K4me3 mark that have shown a significant slight downregulation (-1.44 folds), the levels of the other two modifications H3K27ac and H3K9me3 were not significantly involved in the regulation of the accessibility to the gene (Figure 18).

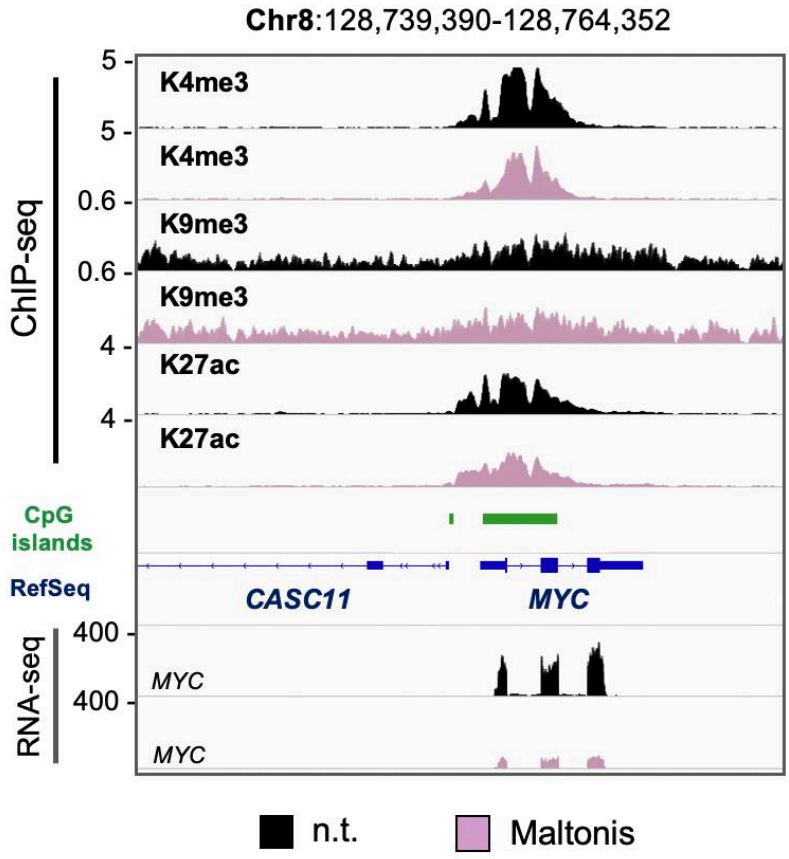

Figure 18. c-MYC locus evaluation in untreated and treated samples. Screenshot of c-MYC locus evaluated by histone marks analyzed through ChIP-seq and transcript expression evaluation from RNA-seq. CpG islands and RefSeq were obtained from UCSC Genome Browser repository. In black is evidenced not treated sample, in lilac maltonis treated cells.

Furthermore, the lower expression was confirmed to be reflected also at the protein levels, where the downregulation is clearly evidenced in the NB4 cells treated as compared to the not treated control in Western Blot (Figure 19). Remarkably, equivalent levels of reduction of the protein have been evidenced in other leukemia cells, such as HL-60, U937, K562, and Jurkat (Figure 19). These data indicated the central role of c-MYC in the remodulation of gene expression induced upon maltonis treatment.

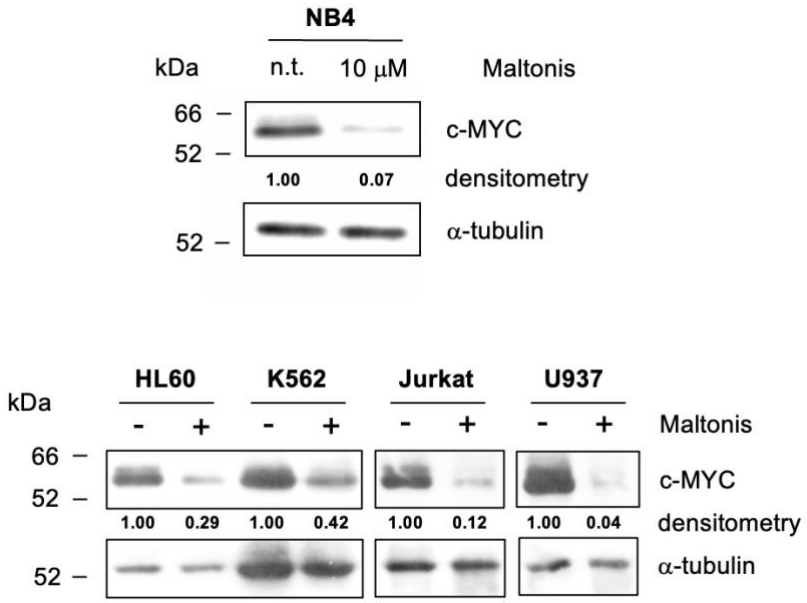

Figure 19. Western Blot evaluation of c-MYC expression after 24 hours treatment. Evaluation of c-MYC expression abundance in NB4 cells (above) and other leukemia cells (below), treated as previously described and then retrieved whole cell lysates for western blot analysis.

Then, to address the question whether this contribution to c-MYC downregulation was induced prematurely at the protein or transcript level, it was carried out an experiment where NB4 cells were plated according to the same experimental conditions of previous experiments and harvested at different time points (2, 4, 8, 24 hours).

RNA and proteins were extracted as described in materials and methods section and then processed: RNA relative abundance was evaluated through qPCR while proteins were immunoblotted against c-MYC (Figure 20). As indicated in figure 20A, RNA abundance is reduced starting from 8 hours to 50 % of the transcript in the treated sample, while no reduction was observed at earlier time points. On the other side, also protein level seems to be affected later by the treatment as shown on transcripts (Figure 20B). In line with these results, c-MYC downregulation appears as a temporal secondary event that remains fundamental to the fully maltonis action on cells during 24 hours of treatment.

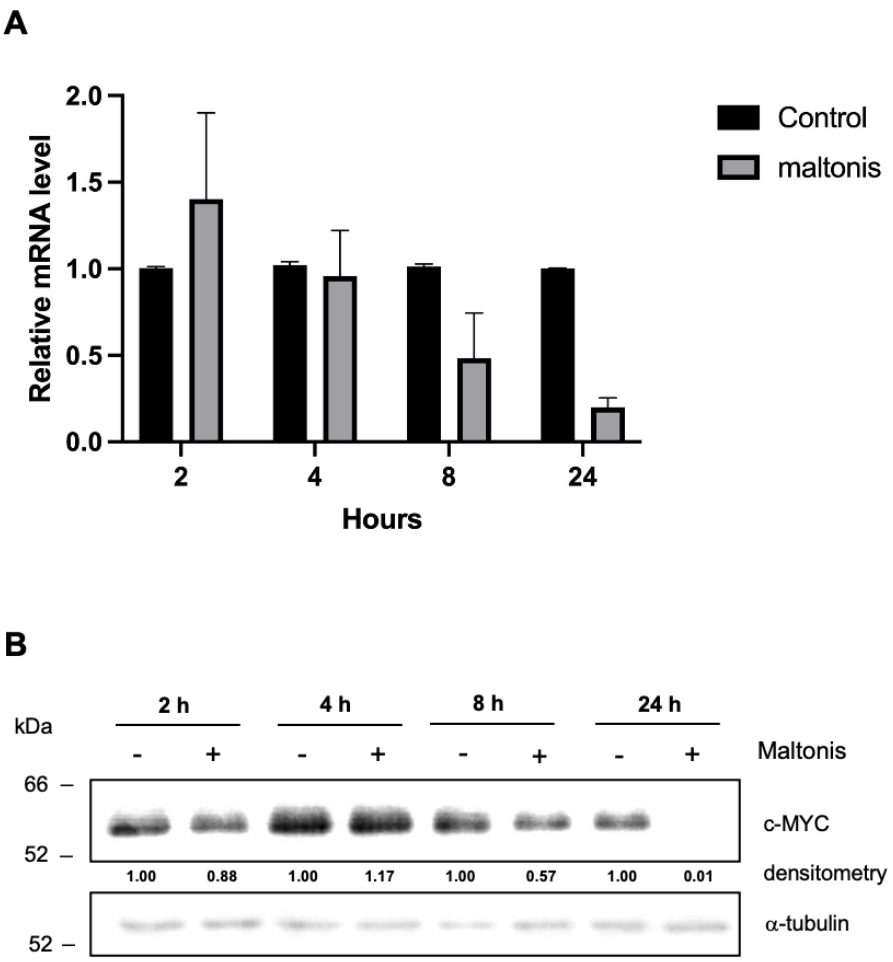

Figure 20. Time course analysis of c-MYC transcript and protein expression level. A) *MYC* transcript analyzed through real-time PCR at different time points in untreated and treated NB4 cells. Data reported as mean value ± standard deviation (SD) of a three independent replicates. **B)** c-MYC abundance levels monitored at reported time points in NB4 cells untreated and treated as reported in previous experiment.

DISCUSSION

Cancer therapies developed in the last two decades have increased the overall survival of patients affected by various tumor types. Despite the promising results obtained and the ongoing advancements in cancer biology research, challenges such as tumor resistance acquisition and lack of targeted therapies remain necessities to be addressed.

In this study, the impact of maltonis, a small molecule member of the hydroxypyrone family of compounds, was investigated in APL blasts. Notably, the molecule has shown hematopoietic cell lines to be the most sensitive (e.g. NB4, U937, HL-60, Jurkat, K562), as also reported by NCI-60 screening, reducing cell survival in the same way at 10 μM dose. Specifically, regarding the APL model NB4 cell line, the molecule is able to induce cell cycle alterations, with an early G2-M phase arrest at the sub-lethal dose tested. This outcome aligns with several reports, where the G2-M arrest is associated with intracellular DNA damage and γ-H2AX incorporation, as already reported in Guerzoni C. *et al.*, 2014, and formation of DNA adducts (Huang R.X. and Zhou P.K., 2020). In a recent published study indeed, the ability of maltonis to form covalent bonds at the chromatin level during cell-free assays, resulting in intermolecular cross linking, was monitored (Amatori S. and Persico G., *et al.*, 2023).

In addition, the treatment triggers a substantial epigenomic remodulation, where different histone post-translational modifications (HTPMs) were strongly affected. In particular, the transcriptional repressive mark H3K9me3 is decreased, as well as H3K9me2, H3K14ac, H3K36me2 and H4ac while other modifications resulted in an increase of their deposition as the transcriptional permissive H3K27ac, H3K4me3 and H3K27me1 marks. These epigenomic remodulation by the molecule is associated with a remodulation of the gene expression profile, with 288 upregulated and 551 downregulated genes identified. Through GSEA, the most significant genes were associated to interferon-like response for upregulated genes; instead G2/M arrest, KRAS-UP signaling, epithelial-mesenchymal transitions and c-MYC target V1/V2 for downregulated genes. As a matter of fact, crossing data from RNA and ChIP-seq have shown how strong correlation of H3K4me3 and H3K27ac DERs with gene expression is, suggesting that these transcriptional permissive markers played a crucial role in the cell response to

treatment. However, bulk H3K9me3 DERs (n = 566) and its decrease was not linked to the gene expression response, since it contributed only to regulate few genes at transcriptional level (n = 20). The vast majority of H3K9me3 DERs were found in distal intergenic regions, unrelated with transcriptional active regions.

The H3K9me3 global downregulation observed might be explained by a decrease of its presence at constitutive heterochromatin enriched sites, later confirmed by RealTime-PCR, where the mark presence is important to silence clustered repeated DNA regions at telomeric, pericentromeric and centromeric regions (Padeken J., et al., 2022).

Those repetitive regions are boosted with transposable elements (TEs) and several papers have discussed how de-silencing of those elements can stimulate an antiviral gene expression response, either via viral mimicry or via cis-acting as enhancer of genes associated with innate response (Drongitis D., *et al.*, 2019; Hale B.G., 2022).

Interestingly, it was found that 91.79 % of TEs (n = 358) were upregulated upon maltonis treatment and that the most representative of the family was the one of long-terminal repeats (LTR) (70 %) with decreased H3K9me3 signal. These LTRs are known to be regulators of gene expression, where they could act as enhancers for nearby genes. In addition, new works have pointed the attention on the molecular regulation of those transposable elements, where the marks observed in TE chromatin are H3K9me3 and H3K27ac, this last one known to be critically important in enhancers action regulation and strongly upregulated by maltonis (Egdginton-White B., *et al.*, 2018; He J., *et al.*, 2019). It could be speculated that maltonis dysregulation of transposable elements, coupled with its action on chromatin and remodulation of the epigenome observed in APL blasts, is the key to the gene expression remodulation as it is plausible that the entire response to treatment is influenced by those elements' activation.

Maltonis-mediated gene expression reprogramming has highlighted c-MYC to be important in the outcome after 24 hours of treatment. Known as the most frequently dysregulated driver of tumorigenesis, *MYC* is one of the most studied genes and, on the other side, one of the most undraggable (Llombart V. and Mansour M.R., 2021). c-MYC participates in a plethora of events and its activity is required for different processes, from regulation of gene expression to protein translation and transcriptional-independent DNA synthesis (Dominguez-Sola D., *et al.*, 2007).

Furthermore, c-MYC is required in hematopoietic stem cells (HSCs) to maintain balance between self-renewal and differentiation. As a matter of fact, c-MYC overexpression is commonly found to be a driver in hematopoietic malignancies, in particular in AML, where it has been proved to be closely related to its development *in vivo* (Luo H., *et al.*, 2005).

Interestingly, in this work, c-MYC has been identified as the master regulator of downregulated genes. From an epigenetic regulation point of view, the gene locus has been investigated and, besides a slight depletion of the H3K4me3 at promoter level, other marks under study do not affect the expression of c-MYC.

Of note was the downregulation of mRNA transcript and protein level in NB4 cells in 24 hours treatment, also observed for other hematopoietic cell lines. Moreover, the treatment affects the expression of the transcript and the protein starting from 8 hours of treatment, meaning that c-MYC is still an important event during exposure to maltonis but not a primary one. These findings are consistent with the fact that leukemic cells are recognized as the most sensitive group of cancer cells to maltonis treatment and exhibit the most higher expression level of *MYC.* This data corroborates the hypothesis that the c-MYC expression decrease is a fundamental step upon maltonis action.

Future efforts will be focused on gaining a deeper understanding of the biological response promoted upon treatment, with particular attention on the intriguing interferon-like response activation. Moreover, future studies on this topic may rely on the timing of this response activation and address the possibility of TEs to be the prompt of cGAS-STING sensing pathway, related to interferon genes activation and triggered by those elements (Zhao Y., *et al.*, 2021). Another thing to address will be the effect of maltonis in chromatin organization, considering its ability to interact with chromatin observed *in vitro*, and if this could impact the regulation of larger domains (e.g. topological associated domain, TAD) after DNA damage, bearing in mind that most of the immune-stimulating genes (ISGs) are grouped in cluster (as many other genes form clusters, such as histones) and located on the same chromosomal location, where they could be subjected to the same epigenetic regulation (Szabo Q., *et al.*, 2020). Lastly, taking into consideration that maltonis could have also an impact in the regulation of bivalent ions, due to similarity with other members of hydroxypyrones family and preliminary chemical approaches,

where it could act as a chelator. Indeed, RNA-seq data have shown that among the most downregulated genes were members belonging to the family of metallothioneins, MT1X, MT1G and MT2A, known to be clustered on the same chromosomal locus (Figure 21A), to play an important role in metal homeostasis and as chaperone for bivalent ions (e.g. Zn^{2+}) (Figure 21B) (Si M. and Lang J., 2018). These genes downregulation may be the cellular response to a competitor for those ions (maltonis) and influence many cellular processes (e.g., methylation) and proteins activities, especially related to epigenetic writers (proteins known to have domains binding bivalent ions, as CXXC or PHD domain), with the final result of a reduced global methylation level (Yusuf A.P., *et al.*, 2021).

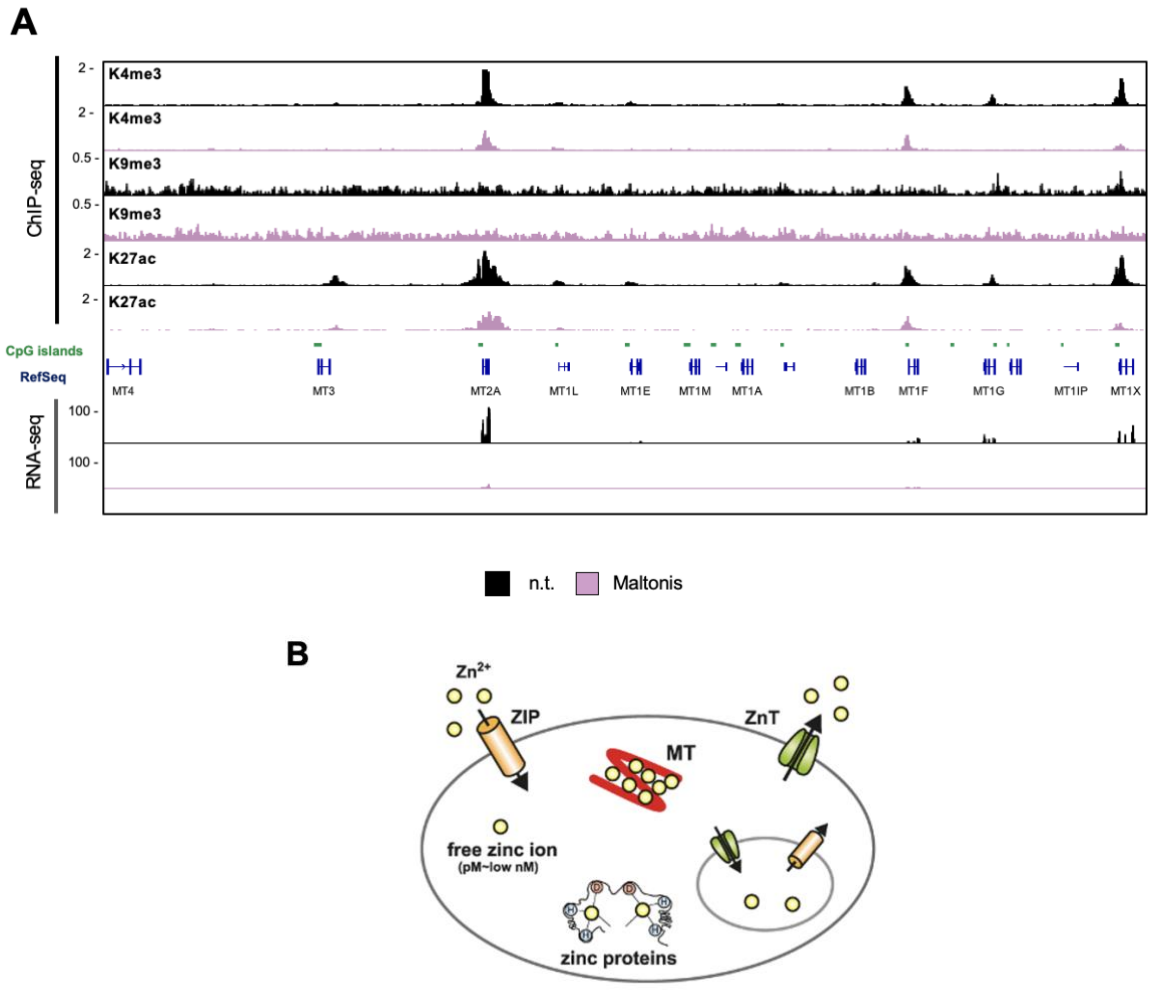

Figure 21. Metallothioneins locus and role in bivalent ions homeostasis. A) Screenshot of all metallothioneins locus on chr. 16 representing a region of 120 kb evaluated by histone marks analyzed through ChIP-seq and transcript expression evaluation from RNA-seq. CpG islands and RefSeq were obtained from UCSC repository. In black the not treated samples, while in lilac the treated with maltonis. **B)** Graphical representation of interplay between zinc transporters and metallothioneins as sequester and reservoir of zinc for zinc

metalloproteins activity, such as various proteins associated with epigenetic modifications (e.g. SETDB1, DOT1L, DNMT3B) (Kimura T. and Kambe T., 2016).

This would be a perfect fit to explain the results obtained in the inhibition of methyltransferases assay, with the consequently diminishing of H3K9me3 tenor, and the MS panel of different histone marks (Figure 9), adding an extra layer to maltonis way of action.

Taken together, this study has demonstrated the ability of maltonis to induce a profound epigenomic reorganization, with a re-assessment of the epigenetic profile and gene expression in NB4 cells. Hence, a possible mechanism of action that could include our analysis and could integrate future efforts is proposed (Figure 22).

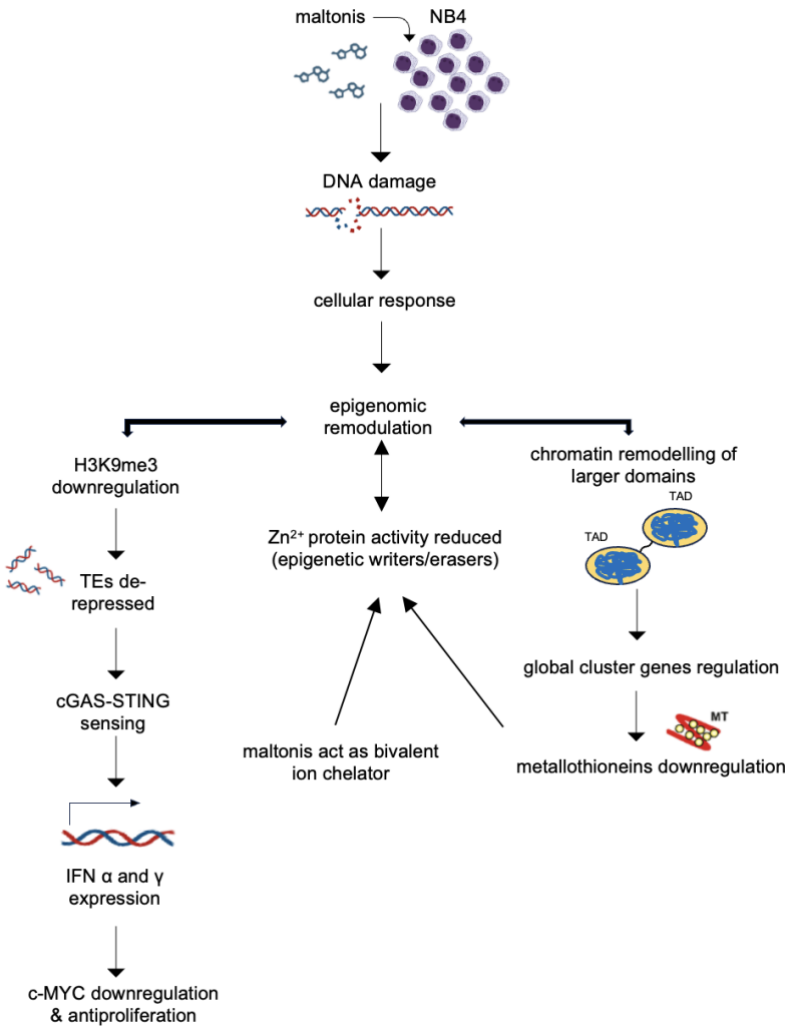

Figure 22. Graphical representation of maltonis mechanism. Proposed model of action after NB4 cell treatment with maltonis that could explain the results obtained, such as the interferon response upregulation and the possible global remodeling of chromatin after DNA damage that could be linked to epigenomic reprogramming and modulation of gene expression observed, may be further explored.

Further investigations are required to expand our knowledge of the compound and possible approaches for delivering the molecule *in vivo* are under investigation.

In conclusion, maltonis has shown the potential to be the most promising small molecule for AML cancer therapy among the hydroxypyrones members derivatives and even new compounds under development are strictly related to maltonis structure.

BIBLIOGRAPHY

Ahmadi, S.E., Rahimi, S., Zarandi, B., Chegeni, R., Safa, M., 2021. MYC: a multipurpose oncogene with prognostic and therapeutic implications in blood malignancies. J Hematol Oncol 14, 121.

Alaskhar Alhamwe, B., Khalaila, R., Wolf, J., von Bülow, V., Harb, H., Alhamdan, F., Hii, C.S., Prescott, S.L., Ferrante, A., Renz, H., Garn, H., Potaczek, D.P., 2018. Histone modifications and their role in epigenetics of atopy and allergic diseases. Allergy, Asthma & Clinical Immunology 14, 39.

Alegría-Torres, J.A., Baccarelli, A., Bollati, V., 2011. Epigenetics and lifestyle. Epigenomics 3, 267–277. https://doi.org/10.2217/epi.11.22

Allis, C.D., Jenuwein, T., 2016. The molecular hallmarks of epigenetic control. Nat Rev Genet 17, 487–500.

Almouzni, G., Cedar, H., 2016. Maintenance of Epigenetic Information. Cold Spring Harb Perspect Biol 8, a019372.

Amatori, S., Ambrosi, G., Fanelli, M., Formica, M., Fusi, V., Giorgi, L., Macedi, E., Micheloni, M., Paoli, P., Pontellini, R., Rossi, P., 2012. Synthesis, Basicity, Structural Characterization, and Biochemical Properties of Two [(3-Hydroxy-4-pyron-2-yl)methyl]amine Derivatives Showing Antineoplastic Features. J Org Chem 77, 2207–2218.

Amatori, S., Bagaloni, I., Macedi, E., Formica, M., Giorgi, L., Fusi, V., Fanelli, M., 2010. Malten, a new synthetic molecule showing in vitro antiproliferative activity against tumour cells and induction of complex DNA structural alterations. Br J Cancer 103, 239–248.

Amatori, S., Persico, G., Cantatore, F., Rusin, M., Formica, M., Giorgi, L., Macedi, E., Casciaro, F., Errico Provenzano, A., Gambardella, S., Noberini, R., Bonaldi, T., Fusi, V., Giorgio, M., Fanelli, M., 2023. Small molecule-induced epigenomic reprogramming of APL blasts leading to antiviral-like response and c-MYC downregulation. Cancer Gene Ther 30, 671-682.

Amatori, S., Persico, G., Paolicelli, C., Hillje, R., Sahnane, N., Corini, F., Furlan, D., Luzi, L., Minucci, S., Giorgio, M., Pelicci, P.G., Fanelli, M., 2018. Epigenomic profiling of archived FFPE tissues by enhanced PAT-ChIP (EPAT-ChIP) technology. Clin Epigenetics 10, 143.

Amatori, S., Tavolaro, S., Gambardella, S., Fanelli, M., 2021a. The dark side of histones: genomic organization and role of oncohistones in cancer. Clin Epigenetics 13, 71.

Anwar-Mohamed, A., El-Kadi, A.O.S., 2007. Induction of cytochrome P450 1a1 by the food flavoring agent, maltol. Toxicology in Vitro 21, 685–690.

Arber, D.A., Orazi, A., Hasserjian, R., Thiele, J., Borowitz, M.J., Le Beau, M.M., Bloomfield, C.D., Cazzola, M., Vardiman, J.W., 2016. The 2016 revision to the World Health Organization classification of myeloid neoplasms and acute leukemia. Blood 127, 2391–2405.

Arshad, J.Z., Hanif, M., 2022. Hydroxypyrone derivatives in drug discovery: from chelation therapy to rational design of metalloenzyme inhibitors. RSC Med Chem 13, 1127–1149.

Ayrapetov, M.K., Gursoy-Yuzugullu, O., Xu, C., Xu, Y., Price, B.D., 2014. DNA double-strand breaks promote methylation of histone H3 on lysine 9 and transient formation of repressive chromatin. Proceedings of the National Academy of Sciences 111, 9169–9174.

Bannister, A.J., Kouzarides, T., 2011. Regulation of chromatin by histone modifications. Cell Res 21, 381–395.

Bar-Sadeh, B., Rudnizky, S., Pnueli, L., Bentley, G.R., Stöger, R., Kaplan, A., Melamed, P., 2020. Unravelling the role of epigenetics in reproductive adaptations to early-life environment. Nat Rev Endocrinol 16, 519–533.

Barve, A., Kumbhar, A., Bhat, M., Joshi, B., Butcher, R., Sonawane, U., Joshi, R., 2009. Mixed-Ligand Copper(II) Maltolate Complexes: Synthesis, Characterization, DNA Binding and Cleavage, and Cytotoxicity. Inorg Chem 48, 9120–9132.

Becker, J.S., Nicetto, D., Zaret, K.S., 2016. H3K9me3-Dependent Heterochromatin: Barrier to Cell Fate Changes. Trends in Genetics 32, 29–41.

Beer, S., Zetterberg, A., Ihrie, R.A., McTaggart, R.A., Yang, Q., Bradon, N., Arvanitis, C., Attardi, L.D., Feng, S., Ruebner, B., Cardiff, R.D., Felsher, D.W., 2004. Developmental Context Determines Latency of MYC-Induced Tumorigenesis. PLoS Biol 2, e332.

Berben, L., Floris, G., Wildiers, H., Hatse, S., 2021. Cancer and Aging: Two Tightly Interconnected Biological Processes. Cancers (Basel) 13, 1400.

Buckberry, S., Liu, X., Poppe, D., Tan, J.P., Sun, G., Chen, J., Nguyen, T.V., de Mendoza, A., Pflueger, J., Frazer, T., Vargas-Landín, D.B., Paynter, J.M., Smits, N., Liu, N., Ouyang, J.F., Rossello, F.J., Chy, H.S., Rackham, O.J.L., Laslett, A.L., Breen, J., Faulkner, G.J., Nefzger, C.M., Polo, J.M., Lister, R., 2023. Transient naive reprogramming corrects hiPS cells functionally and epigenetically. Nature 620, 863-872.

Chammas, P., Mocavini, I., Di Croce, L., 2020. Engaging chromatin: PRC2 structure meets function. Br J Cancer 122, 315–328.

Chen, H., Liu, H., Qing, G., 2018. Targeting oncogenic Myc as a strategy for cancer treatment. Signal Transduct Target Ther 3, 5.

Collas, P., Noer, A., Sørensen, A.L., 2008. Epigenetic Basis for the Differentiation Potential of Mesenchymal and Embryonic Stem Cells. Transfusion Medicine and Hemotherapy 35, 205–215.

Creyghton, M.P., Cheng, A.W., Welstead, G.G., Kooistra, T., Carey, B.W., Steine, E.J., Hanna, J., Lodato, M.A., Frampton, G.M., Sharp, P.A., Boyer, L.A., Young, R.A., Jaenisch, R., 2010. Histone H3K27ac separates active from poised enhancers and predicts developmental state. Proceedings of the National Academy of Sciences 107, 21931–21936.

de Smedt, E., Devin, J., Muylaert, C., Robert, N., Requirand, G., Vlummens, P., Vincent, L., Cartron, G., Maes, K., Moreaux, J., de Bruyne, E., 2021. G9a/GLP targeting in MM promotes autophagy-associated apoptosis and boosts proteasome inhibitor-mediated cell death. Blood Adv 5, 2325–2338.

Di Croce, L., Raker, V.A., Corsaro, M., Fazi, F., Fanelli, M., Faretta, M., Fuks, F., Coco, F. Lo, Kouzarides, T., Nervi, C., Minucci, S., Pelicci, P.G., 2002. Methyltransferase Recruitment and DNA Hypermethylation of Target Promoters by an Oncogenic Transcription Factor. Science (1979) 295, 1079–1082.

Döhner, H., Wei, A.H., Appelbaum, F.R., Craddock, C., DiNardo, C.D., Dombret, H., Ebert, B.L., Fenaux, P., Godley, L.A., Hasserjian, R.P., Larson, R.A., Levine, R.L., Miyazaki, Y., Niederwieser, D., Ossenkoppele, G., Röllig, C., Sierra, J., Stein, E.M., Tallman, M.S., Tien, H.-F., Wang, J., Wierzbowska, A., Löwenberg, B., 2022. Diagnosis and management of AML in adults: 2022 recommendations from an international expert panel on behalf of the ELN. Blood 140, 1345–1377.

Dominguez-Sola, D., Ying, C.Y., Grandori, C., Ruggiero, L., Chen, B., Li, M., Galloway, D.A., Gu, W., Gautier, J., Dalla-Favera, R., 2007. Non-transcriptional control of DNA replication by c-Myc. Nature 448, 445–451.

Dömötör, O., Aicher, S., Schmidlehner, M., Novak, M.S., Roller, A., Jakupec, M.A., Kandioller, W., Hartinger, C.G., Keppler, B.K., Enyedy, É.A., 2014. Antitumor pentamethylcyclopentadienyl rhodium complexes of maltol and allomaltol: Synthesis, solution speciation and bioactivity. J Inorg Biochem 134, 57–65.

Dong, Y., Shi, O., Zeng, Q., Lu, X., Wang, W., Li, Y., Wang, Q., 2020. Leukemia incidence trends at the global, regional, and national level between 1990 and 2017. Exp Hematol Oncol 9, 14.

Drongitis, D., Aniello, F., Fucci, L., Donizetti, A., 2019. Roles of Transposable Elements in the Different Layers of Gene Expression Regulation. Int J Mol Sci 20, 5755.

Durbin, A., Wang, T., Wimalasena, V., Zimmerman, M., Li, D., Dharia, N., Mariani, L., Shendy, N., Nance, S., Patel, A., Shao, Y., Mundada, M., Maxham, L., Park, P., Sigua, L., Morita, K., Conway, A., Robichaud, A., Perez-Atayde, A., Bikowitz, M., Quinn, T., Wiest, O., Easton, J., Schönbrunn, E., Bulyk, M., Abraham, B., Stegmaier, K., Look, A., Qi, J., 2022. EP300 Selectively Controls the Enhancer Landscape of MYCN Amplified Neuroblastoma. Cancer Discovery 12, 730-751.

Edginton-White, B., Cauchy, P., Assi, S.A., Hartmann, S., Riggs, A.G., Mathas, S., Cockerill, P.N., Bonifer, C., 2019. Global long terminal repeat activation participates in establishing the unique gene expression programme of classical Hodgkin lymphoma. Leukemia 33, 1463–1474

Fanelli, M., Caprodossi, S., Ricci-Vitiani, L., Porcellini, A., Tomassoni-Ardori, F., Amatori, S., Andreoni, F., Magnani, M., De Maria, R., Santoni, A., Minucci, S., Pelicci, P.G., 2008b. Loss of pericentromeric DNA methylation pattern in human glioblastoma is associated with altered DNA methyltransferases expression and involves the stem cell compartment. Oncogene 27, 358–365.

Fanelli, M., and Fusi, V. (2010) PCT Int. Appl. WO 2010061282 A1 20100603.

Fennell, K.A., Bell, C.C., Dawson, M.A., 2019. Epigenetic therapies in acute myeloid leukemia: where to from here? Blood 134, 1891–1901.

Ferlay, J., Colombet, M., Soerjomataram, I., Parkin, D.M., Piñeros, M., Znaor, A., Bray, F., 2021. Cancer statistics for the year 2020: An overview. Int J Cancer 149, 778–789.

Fiorillo, M., Tóth, F., Brindisi, M., Sotgia, F., Lisanti, M.P., 2020. Deferiprone (DFP) Targets Cancer Stem Cell (CSC) Propagation by Inhibiting Mitochondrial Metabolism and Inducing ROS Production. Cells 9, 1529.

Gabay, M., Li, Y., Felsher, D.W., 2014. MYC Activation Is a Hallmark of Cancer Initiation and Maintenance. Cold Spring Harb Perspect Med 4, a014241–a014241.

Gaggioli, V., Lo, C., Reverón-Gómez, N., Jasencakova, Z., Domenech, H., Nguyen, H., Sidoli, S., Tvardovskiy, A., Uruci, S., Slotman, J., Chai, Y., Gonçalves, J., Manolika, E., Jensen, O., Wheeler, D., Sridharan, S., Chakrabarty, S., Demmers, J., Kanaar, R., Groth, A., Taneja, N., 2023. Dynamic de novo heterochromatin assembly and disassembly at replication forks ensures fork stability. Nature Cell Biol 25, 1017-1032.

Gang, A.O., Frøsig, T.M., Brimnes, M.K., Lyngaa, R., Treppendahl, M.B., Grønbæk, K., Dufva, I.H., Straten, P. thor, Hadrup, S.R., 2014. 5-Azacytidine treatment sensitizes tumor cells to T-cell mediated cytotoxicity and modulates NK cells in patients with myeloid malignancies. Blood Cancer J 4, e197–e197.

Goldman, S.L., Hassan, C., Khunte, M., Soldatenko, A., Jong, Y., Afshinnekoo, E., Mason, C.E., 2019. Epigenetic Modifications in Acute Myeloid Leukemia: Prognosis, Treatment, and Heterogeneity. Front Genet 10.

Greer, E.L., Shi, Y., 2012. Histone methylation: a dynamic mark in health, disease and inheritance. Nat Rev Genet 13, 343–357.

Guerzoni, C., Amatori, S., Giorgi, L., Manara, M.C., Landuzzi, L., Lollini, P.-L., Tassoni, A., Balducci, M., Manfrini, M., Pratelli, L., Serra, M., Picci, P., Magnani, M., Fusi, V., Fanelli, M., Scotlandi, K., 2014. An aza-macrocycle containing maltolic side-arms (maltonis) as potential drug against human pediatric sarcomas. BMC Cancer 14, 137.

Hale, B.G., 2022. Antiviral immunity triggered by infection-induced host transposable elements. Curr Opin Virol 52, 211–216.

Hanahan, D., Weinberg, R.A., 2011. Hallmarks of Cancer: The Next Generation. Cell 144, 646–674.

Harvey, R.S.J., Reffitt, D.M., Doig, L.A., Meenan, J., Ellis, R.D., Thompson, R.P.H., Powell, J.J., 1998. Ferric trimaltol corrects iron deficiency anaemia in patients intolerant of iron. Aliment Pharmacol Ther 12, 845–848.

He, J., Fu, X., Zhang, M., He, F., Li, W., Abdul, M.Md., Zhou, J., Sun, L., Chang, C., Li, Y., Liu, H., Wu, K., Babarinde, I.A., Zhuang, Q., Loh, Y.-H., Chen, J., Esteban, M.A., Hutchins, A.P., 2019. Transposable elements are regulated by context-specific patterns of chromatin marks in mouse embryonic stem cells. Nat Commun 10, 34.

Hoffman, B., Amanullah, A., Shafarenko, M., Liebermann, D.A., 2002. The proto-oncogene c-myc in hematopoietic development and leukemogenesis. Oncogene 21, 3414–3421.

Hou, J., He, Z., Liu, T., Chen, D., Wang, B., Wen, Q., Zheng, X., 2022. Evolution of Molecular Targeted Cancer Therapy: Mechanisms of Drug Resistance and Novel Opportunities Identified by CRISPR-Cas9 Screening. Front Oncol 12.

Howe, F., Fischl, H., Murray, S., Mellor, J., 2017. Is H3K4me3 instructive for transcritption activation?. BioEssays 39, e201600095.

Hu, D., Shilatifard, A., 2016. Epigenetics of hematopoiesis and hematological malignancies. Genes Dev 30, 2021–2041.

Huang, R.-X., Zhou, P.-K., 2020. DNA damage response signaling pathways and targets for radiotherapy sensitization in cancer. Signal Transduct Target Ther 5, 60.

Jenuwein, T., Allis, C.D., 2001b. Translating the Histone Code. Science (1979) 293, 1074–1080.

Jin, B., Li, Y., Robertson, K.D., 2011. DNA Methylation: Superior or Subordinate in the Epigenetic Hierarchy? Genes Cancer 2, 607–617.

Kandioller, W., Hartinger, C.G., Nazarov, A.A., Kasser, J., John, R., Jakupec, M.A., Arion, V.B., Dyson, P.J., Keppler, B.K., 2009. Tuning the anticancer activity of maltol-derived ruthenium complexes by derivatization of the 3-hydroxy-4-pyrone moiety. J Organomet Chem 694, 922–929.

Karakaya, G., Türe, A., Özdemir, A., Özçelik, B., Aytemir, M., 2022. Synthesis and molecular modeling of some novel hydroxypyrone derivatives as antidermatophytic agents. J Heterocycl Chem 59, 1801–1812.

Khodaverdian, V., Tapadar, S., MacDonald, I.A., Xu, Y., Ho, P.-Y., Bridges, A., Rajpurohit, P., Sanghani, B.A., Fan, Y., Thangaraju, M., Hathaway, N.A., Oyelere, A.K., 2019. Deferiprone: Pan-selective Histone Lysine Demethylase Inhibition Activity and Structure Activity Relationship Study. Sci Rep 9, 4802.

Kimura, T., Kambe, T. 2016. The Functions of Metallothionein and ZIP and ZnT Transporters: An Overview and Perspective. Int J Mol Sci. 17(3):336.

Klemm, S.L., Shipony, Z., Greenleaf, W.J., 2019. Chromatin accessibility and the regulatory epigenome. Nat Rev Genet 20, 207–220.

Kumar, M., Rani, K., 2023. Epigenomics in stress tolerance of plants under the climate change. Mol Biol Rep.

Lee, S., Schmitt, C.A., 2019. The dynamic nature of senescence in cancer. Nat Cell Biol 21, 94–101.

León, I.E., Butenko, N., Di Virgilio, A.L., Muglia, C.I., Baran, E.J., Cavaco, I., Etcheverry, S.B., 2014. Vanadium and cancer treatment: Antitumoral mechanisms of three oxidovanadium(IV) complexes on a human osteosarcoma cell line. J Inorg Biochem 134, 106–117.

Liu, X., Wang, C., Liu, W., Li, J., Li, C., Kou, X., Chen, J., Zhao, Y., Gao, H., Wang, H., Zhang, Y., Gao, Y., Gao, S., 2016. Distinct features of H3K4me3 and H3K27me3 chromatin domains in pre-implantation embryos. Nature 537, 558-562.

Llombart, V., Mansour, M.R., 2022. Therapeutic targeting of “undruggable” MYC. EBioMedicine 75, 103756.

Luo, H., Li, Q., O’Neal, J., Kreisel, F., Le Beau, M.M., Tomasson, M.H., 2005. c-Myc rapidly induces acute myeloid leukemia in mice without evidence of lymphoma-associated antiapoptotic mutations. Blood 106, 2452–2461.

Macedi, E., Paderni, D., Formica, M., Conti, L., Fanelli, M., Giorgi, L., Amatori, S., Ambrosi, G., Valtancoli, B., Fusi, V., 2020. Playing with Structural Parameters: Synthesis and

Characterization of Two New Maltol-Based Ligands with Binding and Antineoplastic Properties. Molecules 25, 943.

Madden, S.K., de Araujo, A.D., Gerhardt, M., Fairlie, D.P., Mason, J.M., 2021. Taking the Myc out of cancer: toward therapeutic strategies to directly inhibit c-Myc. Mol Cancer 20, 3.

Marsano, R.M., Dimitri, P., 2022. Constitutive Heterochromatin in Eukaryotic Genomes: A Mine of Transposable Elements. Cells 11, 761.

Mattei, A.L., Bailly, N., Meissner, A., 2022. DNA methylation: a historical perspective. Trends in Genetics 38, 676–707.

Mehdipour, P., Santoro, F., Minucci, S., 2015. Epigenetic alterations in acute myeloid leukemias. FEBS Journal 282, 1786–1800.

Miller, D.M., Thomas, S.D., Islam, A., Muench, D., Sedoris, K., 2012. c-Myc and Cancer Metabolism. Clinical Cancer Research 18, 5546–5553.

Molyneux, E.M., Rochford, R., Griffin, B., Newton, R., Jackson, G., Menon, G., Harrison, C.J., Israels, T., Bailey, S., 2012. Burkitt's lymphoma. The Lancet 379, 1234–1244.

Monaghan, L., Massett, M.E., Bunschoten, R.P., Hoose, A., Pirvan, P.A., Liskamp, R.M.J., Jørgensen, H.G., Huang, X., 2019. The Emerging Role of H3K9me3 as a Potential Therapeutic Target in Acute Myeloid Leukemia. Front Oncol.

Moore, L.D., Le, T., Fan, G., 2013. DNA Methylation and Its Basic Function. Neuropsychopharmacology 38, 23–38.

Murakami, K., Ishida, K., Watakabe, K., Tsubouchi, R., Naruse, M., Yoshino, M., 2006. Maltol/iron-mediated apoptosis in HL60 cells: Participation of reactive oxygen species. Toxicol Lett 161, 102–107.

Nilsson, J.A., Cleveland, J.L., 2003. Myc pathways provoking cell suicide and cancer. Oncogene 22, 9007–9021.

Ntorla, A., Burgoyne, J.R., 2021b. The Regulation and Function of Histone Crotonylation. Front Cell Dev Biol 9.

Okumura, S., Konishi, Y., Narukawa, M., Sugiura, Y., Yoshimoto, S., Arai, Y., Sato, S., Yoshida, Y., Tsuji, S., Uemura, K., Wakita, M., Matsudaira, T., Matsumoto, T., Kawamoto, S., Takahashi, A., Itatani, Y., Miki, H., Takamatsu, M., Obama, K., Takeuchi, K., Suematsu, M., Ohtani, N., Fukunaga, Y., Ueno, M., Sakai, Y., Nagayama, S., Hara, E., 2021. Gut bacteria identified in colorectal cancer patients promote tumourigenesis via butyrate secretion. Nat Commun 12, 5674.

Padeken, J., Methot, S.P., Gasser, S.M., 2022. Establishment of H3K9-methylated heterochromatin and its functions in tissue differentiation and maintenance. Nat Rev Mol Cell Biol 23, 623–640.

Pan, X.-N., Chen, J.-J., Wang, L.-X., Xiao, R.-Z., Liu, L.-L., Fang, Z.-G., Liu, Q., Long, Z.-J., Lin, D.-J., 2014. Inhibition of c-Myc Overcomes Cytotoxic Drug Resistance in Acute Myeloid Leukemia Cells by Promoting Differentiation. PLoS One 9, e105381.

Pelengaris, S., Khan, M., Evan, G., 2002. c-MYC: more than just a matter of life and death. Nat Rev Cancer 2, 764–776.

Quina, A.S., Buschbeck, M., Di Croce, L., 2006a. Chromatin structure and epigenetics. Biochem Pharmacol 72, 1563–1569.

Quina, A.S., Buschbeck, M., Di Croce, L., 2006b. Chromatin structure and epigenetics. Biochem Pharmacol 72, 1563–1569.

Riggs, A.D., Xiong, Z., 2004. Methylation and epigenetic fidelity. Proceedings of the National Academy of Sciences 101, 4–5.

Rodríguez-Paredes, M., Esteller, M., 2011. Cancer epigenetics reaches mainstream oncology. Nat Med 17, 330–339.

Satoh, K., Yachida, S., Sugimoto, M., Oshima, M., Nakagawa, T., Akamoto, S., Tabata, S., Saitoh, K., Kato, K., Sato, S., Igarashi, K., Aizawa, Y., Kajino-Sakamoto, R., Kojima, Y., Fujishita, T., Enomoto, A., Hirayama, A., Ishikawa, T., Taketo, M.M., Kushida, Y., Haba, R., Okano, K., Tomita, M., Suzuki, Y., Fukuda, S., Aoki, M., Soga, T., 2017. Global metabolic reprogramming of colorectal cancer occurs at adenoma stage and is induced by MYC. Proceedings of the National Academy of Sciences 114.

Schmidt, C., Allen, S., Kopyt, N., Pergola, P., 2021. Iron Replacement Therapy with Oral Ferric Maltol: Review of the Evidence and Expert Opinion. J Clin Med 10, 4448.

Sekeres, M.A., Guyatt, G., Abel, G., Alibhai, S., Altman, J.K., Buckstein, R., Choe, H., Desai, P., Erba, H., Hourigan, C.S., LeBlanc, T.W., Litzow, M., MacEachern, J., Michaelis, L.C., Mukherjee, S., O'Dwyer, K., Rosko, A., Stone, R., Agarwal, A., Colunga-Lozano, L.E., Chang, Y., Hao, Q., Brignardello-Petersen, R., 2020. American Society of Hematology 2020 guidelines for treating newly diagnosed acute myeloid leukemia in older adults. Blood Adv 4, 3528–3549.

Shoemaker, R.H., 2006. The NCI60 human tumour cell line anticancer drug screen. Nat Rev Cancer 6, 813–823.

Si, M., Lang, J. 2018 The roles of metallothioneins in carcinogenesis. J Hematol Oncol. 11(1):107.

Sidhwani, P., Straight, A., 2023. Epigenetic inheritance and boundary maintenance at human centromeres. Current Opin in Struct Biol 82, 102694.

Strippoli, A., Cocomazzi, A., Basso, M., Cenci, T., Ricci, R., Pierconti, F., Cassano, A., Fiorentino, V., Barone, C., Bria, E., Ricci-Vitiani, L., Tortora, G., Larocca, L.M., Martini, M., 2020. c-MYC Expression Is a Possible Keystone in the Colorectal Cancer Resistance to EGFR Inhibitors. Cancers (Basel) 12, 638.

Szabo, Q., Donjon, A., Jerković, I., Papadopoulos, GL., Cheutin, T., Bonev, B., Nora, EP., Bruneau, BG., Bantignies, F., Cavalli, G. 2020. Regulation of single-cell genome organization into TADs and chromatin nanodomains. Nat Genet. 52(11):1151-1157.

Tarakhovsky, A., 2010. Tools and landscapes of epigenetics. Nat Immunol. 11, 565–568.

Taylor, J., Xiao, W., Abdel-Wahab, O., 2017a. Diagnosis and classification of hematologic malignancies on the basis of genetics. Blood 130, 410–423.

Taylor, J., Xiao, W., Abdel-Wahab, O., 2017b. Diagnosis and classification of hematologic malignancies on the basis of genetics. Blood 130, 410–423.

Toso, L., Crisponi, G., Nurchi, V.M., Crespo-Alonso, M., Lachowicz, J.I., Santos, M.A., Marques, S.M., Niclós-Gutiérrez, J., González-Pérez, J.M., Domínguez-Martín, A., Choquesillo-Lazarte, D., Szewczuk, Z., 2013. A family of hydroxypyrone ligands designed and synthesized as iron chelators. J Inorg Biochem 127, 220–231.

Turpin, M., Salbert, G., 2022. 5-methylcytosine turnover: Mechanisms and therapeutic implications in cancer. Front Mol Biosci 9.

Wang, H., Fan, Z., Shliaha, P., Miele, M., Hendrickson, R., Jiang, X., Helin, K., 2023. H3K4me3 regulates RNA polymerase II promoter-proximal pause-release. Nature 615, 339-348.

Wood, J.G., Helfand, S.L., 2013. Chromatin structure and transposable elements in organismal aging. Front Genet 4.

Wu, K., Fan, D., Zhao, H., Liu, Z., Hou, Z., Tao, W., Yu, G., Yuan, S., Zhu, X., Kang, M., Tian, Y., Chen, Z., Liu, J., Gao, L., 2023. Cell Discovery 9, 29.

Wu, S., Powers, S., Zhu, W., Hannun, Y.A., 2016. Substantial contribution of extrinsic risk factors to cancer development. Nature 529, 43–47.

Wu, S.C., Zhang, Y., 2010. Active DNA demethylation: many roads lead to Rome. Nat Rev Mol Cell Biol 11, 607–620.

Wu, X., Zhang, Y., 2017. TET-mediated active DNA demethylation: mechanism, function and beyond. Nat Rev Genet 18, 517–534.

Xu, J., Chen, Y., Olopade, O.I., 2010. MYC and Breast Cancer. Genes Cancer 1, 629–640.

Yan, Y.-L., Miller, M.T., Cao, Y., Cohen, S.M., 2009. Synthesis of hydroxypyrone- and hydroxythiopyrone-based matrix metalloproteinase inhibitors: Developing a structure–activity relationship. Bioorg Med Chem Lett 19, 1970–1976.

Yusuf, A.P., Abubakar, M.B., Malami, I., Ibrahim, K.G., Abubakar, B., Bello, M.B., Qusty, N., Elazab, S.T., Imam, M.U., Alexiou, A., Batiha, G.E. 2021. Zinc Metalloproteins in Epigenetics and Their Crosstalk. Life (Basel). 11(3):186.

Zeng, Y., Chen, T., 2019. DNA Methylation Reprogramming during Mammalian Development. Genes (Basel) 10, 257.

Zhao, Y., Oreskovic, E., Zhang, Q., Lu, Q., Gilman, A., Lin, YS., He, J., Zheng, Z., Lu, JY., Lee, J., Ke, Z., Ablaeva, J., Sweet, MJ., Horvath, S., Zhang, Z., Nevo, E., Seluanov, A.,

Gorbunova, V. 2021. Transposon-triggered innate immune response confers cancer resistance to the blind mole rat. Nat Immunol. 22(10):1219-1230.

Zhong, L., Li, Y., Xiong, L., Wang, W., Wu, M., Yuan, T., Yang, W., Tian, C., Miao, Z., Wang, T., Yang, S., 2021. Small molecules in targeted cancer therapy: advances, challenges, and future perspectives. Signal Transduct Target Ther 6, 201.